

BINARY PARTICLE SWARM OPTIMIZATION ALGORITHM FOR OPTIMIZATION OF STEEL
STRUCTURE



A Thesis Submitted in Partial Fulfillment of the Requirements
for the Degree of Master of Engineering in Civil Engineering

Department of Civil Engineering

FACULTY OF ENGINEERING

Chulalongkorn University

Academic Year 2020

Copyright of Chulalongkorn University

การออกแบบโครงสร้างเหล็กที่เหมาะสมด้วยระเบียบวิธีวิภาคของกลุ่มอนุภาค



วิทยานิพนธ์นี้เป็นส่วนหนึ่งของการศึกษาตามหลักสูตรปริญญาวิศวกรรมศาสตรมหาบัณฑิต

สาขาวิชาวิศวกรรมโยธา ภาควิชาวิศวกรรมโยธา

คณะวิศวกรรมศาสตร์ จุฬาลงกรณ์มหาวิทยาลัย

ปีการศึกษา 2563

ลิขสิทธิ์ของจุฬาลงกรณ์มหาวิทยาลัย

Thesis Title BINARY PARTICLE SWARM OPTIMIZATION ALGORITHM
FOR OPTIMIZATION OF STEEL STRUCTURE

By Miss Atitaya Chaiwongnoi

Field of Study Civil Engineering

Thesis Advisor Associate Professor SAWEKCHAI TANGARAMVONG

Accepted by the FACULTY OF ENGINEERING, Chulalongkorn University in
Partial Fulfillment of the Requirement for the Master of Engineering

----- Dean of the FACULTY OF
ENGINEERING
(Professor SUPOT TEACHAVORASINSKUN)

THESIS COMMITTEE

----- Chairman
(Associate Professor WITHIT PANSUK)

----- Thesis Advisor
(Associate Professor SAWEKCHAI TANGARAMVONG)

----- External Examiner
(Assistant Professor Pakawat Sancharoen)

จุฬาลงกรณ์มหาวิทยาลัย
CHULALONGKORN UNIVERSITY

อาทิตยา ไชยวงศ์น้อย : การออกแบบโครงสร้างเหล็กที่เหมาะสมด้วยระเบียบวิธีวิภาค
 ของกลุ่มอนุภาค. (BINARY PARTICLE SWARM OPTIMIZATION ALGORITHM FOR
 OPTIMIZATION OF STEEL STRUCTURE) อ.ที่ปรึกษาหลัก : รศ. ดร.เสวกชัย ตั้งอร่าม
 วงศ์

บทความนี้ศึกษาระเบียบวิธีวิภาคของกลุ่มอนุภาค (BPSO) โดยในส่วนที่หนึ่งเป็น
 การศึกษาเพื่อหาน้ำหนักความเฉื่อยของอนุภาคที่ดีที่สุดจากกลุ่มตัวอย่างที่ศึกษา และในส่วนที่สอง
 เป็นการหาค่าเหมาะสมของพื้นที่หน้าตัดของโครงสร้างเหล็กที่กระทำโดยน้ำหนักบรรทุกทุกแนวตั้ง
 และแนวขวางเพื่อให้ได้น้ำหนักโครงสร้างที่น้อยที่สุด โดยโครงสร้างเหล็กที่ศึกษามีทั้งหมด 2
 กรณีศึกษา ได้แก่ โครงสร้างแบบไม่มีระบบค้ำยันและโครงสร้างแบบมีระบบค้ำยันรูปแบบตัวเอ็กซ์
 โดยในโครงสร้างแบบมีระบบค้ำยันยังศึกษาเพิ่มเติมในอิทธิพลของการแบ่งกลุ่มชิ้นส่วน โดยมีการ
 แบ่งกลุ่มชิ้นส่วนให้มีจำนวนกลุ่มมากกว่าการแบ่งกลุ่มเดิม การออกแบบโครงสร้างเป็นไปตาม
 ข้อกำหนดของ AISC ผลการศึกษาในส่วนแรกพบว่าน้ำหนักความเฉื่อยที่ดีที่สุด คือ น้ำหนักความ
 เฉื่อยแบบคงที่ที่มีค่า 0.98 และผลการศึกษาในส่วนนี้สองพบว่า BPSO สามารถหาน้ำหนัก
 โครงสร้างแบบไม่มีระบบค้ำยันได้น้อยที่สุดเมื่อเปรียบเทียบกับระเบียบวิธีที่ได้ศึกษาก่อนหน้านี้
 ยกเว้น โครงสร้างสามแฉกยี่สิบสี่ชั้นที่ระเบียบวิธีนี้ได้หาน้ำหนักที่มากกว่า ในโครงสร้างแบบมีระบบค้ำ
 ยัน ทุกตัวอย่างศึกษาให้น้ำหนักที่น้อยกว่าโครงสร้างแบบไม่มีระบบค้ำยัน การศึกษาอิทธิพลการ
 แบ่งกลุ่มพบว่าผลลัพธ์มีความขัดแย้งกันโดยในโครงสร้างหนึ่งแฉกยี่สิบสี่ชั้น การแบ่งกลุ่มที่ละเอียด
 กว่าทำให้ได้น้ำหนักโครงสร้างที่น้อยกว่า แต่โครงสร้างสามแฉกยี่สิบสี่ชั้นกลับให้ผลที่ตรงกันข้าม

จุฬาลงกรณ์มหาวิทยาลัย
 CHULALONGKORN UNIVERSITY

สาขาวิชา วิศวกรรมโยธา

ปีการศึกษา 2563

ลายมือชื่อนิสิต

ลายมือชื่อ อ.ที่ปรึกษาหลัก

6170335521 : MAJOR CIVIL ENGINEERING

KEYWORD: Binary Particle Swarm Optimization, Structural Optimization, Inertia Weight, Steel Structure, Bracing System

Atitaya Chaiwongnoi : BINARY PARTICLE SWARM OPTIMIZATION ALGORITHM FOR OPTIMIZATION OF STEEL STRUCTURE. Advisor: Assoc. Prof. SAWEKCHAI TANGARAMVONG

This research studies on the performance of Binary Particle Swarm Optimization (BPSO) algorithm. The first part is finding the best inertia weight of BPSO from various types of inertia weight. The second part is optimizing the cross-sectional area of steel structures and topology of bracing system under vertical and lateral load. The structures studied in the research include unbraced frames and X-braced frames. Moreover, the braced frame also investigates the influence of the classification groups of elements. The elements are classified into finer groups than the original group. The design of the structure follows the AISC code. From the investigation in the first part, a constant inertia weight of 0.98 is the best. In the second part, minimum weights of unbraced frames using BPSO are the lowest weight, except three-bays, twenty-four stories frame. For braced frames with original grouping, all examples get a lower weight than the unbraced frames. For studying the influence of group, the results of the two examples are contradictory. One bay, ten stories frame with new group has a minimum weight less than the original while three-bays but twenty-four stories frame is opposite.

Field of Study: Civil Engineering

Student's Signature

Academic Year: 2020

Advisor's Signature

ACKNOWLEDGEMENTS

First of all, I would like to express my deepest appreciation to my committee, Assoc. Prof. Sawekchai Tangaramvong, for his valuable and constructive advice during my research process. My research would not have been possible without his support and nurturing.

Besides my advisor, I would like to thank my committee members for their insightful comments.

I would like to thank my family for their strong support and encouragement.

I thank my friend for their help and motivation.

My grateful thanks to faculty staff working at the department of civil engineering for their helpfulness.

Atitaya Chaiwongnoi

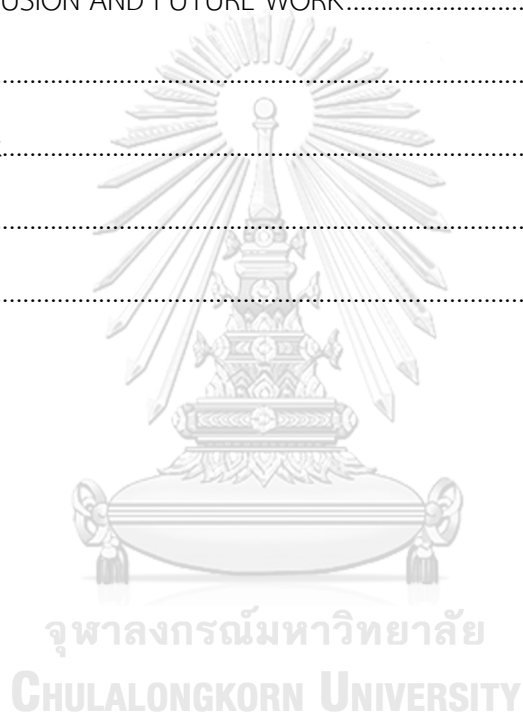


TABLE OF CONTENTS

	Page
.....	iii
ABSTRACT (THAI)	iii
.....	iv
ABSTRACT (ENGLISH)	iv
ACKNOWLEDGEMENTS	v
TABLE OF CONTENTS	vi
LIST OF TABLES	ix
LIST OF FIGURES.....	x
CHAPTER 1 INTRODUCTION	1
1.1 Background.....	1
1.2 Research Objectives.....	2
1.3 Scopes	3
1.4 Methodology.....	4
CHAPTER 2 LITERATURE REVIEW.....	5
2.1 Binary Particle Swarm Optimization (BPSO).....	5
2.1.1 Background of BPSO	5
2.1.2 Previous PSO Articles on Inertia Weight	7
2.1.3 Previous BPSO Articles	7
2.2 Structural Analysis	8
2.2.1 General.....	8
2.2.2 Stiffness Matrix Analysis	8

2.2.3 Amplified First-Order Elastic Analysis by AISC.....	13
2.3 Unbraced Frame VS Braced Frame Design against Lateral Load	14
2.4 Steel Structural Optimization using Meta-heuristic Algorithm.....	15
CHAPTER 3 BINARY PARTICLE SWARM OPTIMIZATION ALGORITHM.....	16
3.1 General.....	16
3.2 BPSO Parameters	16
3.2.1 Initial Parameters.....	16
3.2.2 Inertia Weight	16
3.2.3 Stopping Criteria	17
3.3 The Transformation between Binary Space and Real Number Space	17
3.4 BPSO Processes	19
CHAPTER 4 STRUCTURAL OPTIMIZATION.....	21
4.1 General.....	21
4.2 Objective and Constrained Functions.....	21
4.3 AISC-LRFD Design	22
4.3.1 Story Drift Design.....	22
4.3.2 Strength Design	22
4.3.2.1 Axial Strength Design	22
4.3.2.2 Flexural Strength Design	24
4.4 Planer Steel Frame Optimization.....	27
4.4.1 Element Connection.....	27
4.4.2 Available Section for Optimization	28
4.4.3 Loads	29
CHAPTER 5 NUMERICAL EXAMPLES	30

5.1 General	30
5.2 Inertia Weight Studies	30
5.3 Structural Optimization	33
5.3.1 Two-Bays, Three-Stories Frame	34
5.3.2 One-bay, Ten-Stories Frame.....	36
5.3.3 Three-Bays, Twenty-Four-Stories Frame.....	45
CHAPTER 6 CONCLUSION AND FUTURE WORK.....	56
6.1 Conclusion.....	56
6.2 Future Work.....	59
REFERENCES.....	61
VITA	65



LIST OF TABLES

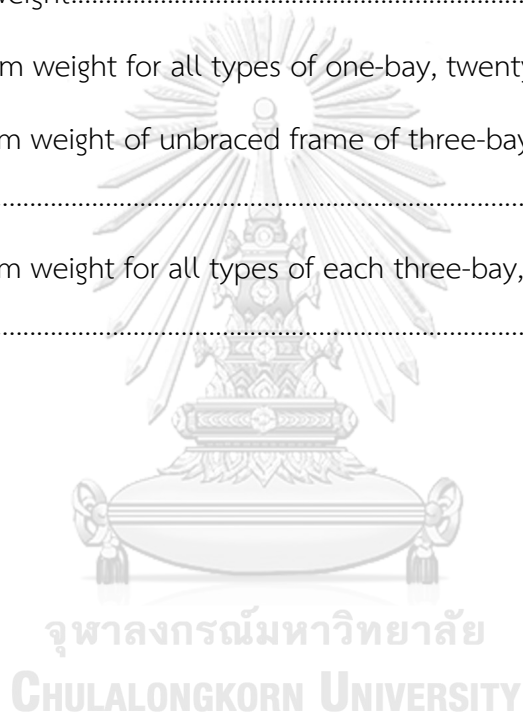
	Page
Table 4.1 Available bending moment of section.....	26
Table 4.2 Available AISC section data.....	28
Table 5.1 Benchmark functions with range and optimal value.....	30
Table 5.2 Minimum fitness of inertia weight on benchmark functions.....	32
Table 5.3 Standard deviation of inertia weight on benchmark functions.....	32
Table 5.4 Two-bays, three-stories frame design.....	35
Table 5.5 Types and condition of structure for one-bay, ten-stories frame.....	37
Table 5.6 One-bay, ten-stories frame design (No.1).....	38
Table 5.7 One-bay, ten-stories frame design (No.2).....	39
Table 5.8 One-bay, ten-stories frame design (No.3).....	40
Table 5.9 One-bay, ten-stories frame design (No.4).....	41
Table 5.10 Types and condition for three-bays, twenty-four-stories frame.....	46
Table 5.11 Three-bays, twenty-four-stories design (No.1).....	47
Table 5.12 Three-bays, twenty-four-stories frame design (No.2).....	50
Table 5.13 Three-bays, twenty-four-stories frame design (No.3).....	51

LIST OF FIGURES

	Page
Figure 1.1 Graph indicates local and global optima	1
Figure 1.2 Framework (a) unbrace structure (b) braced structure	2
Figure 2.1 Updating PSO particle	5
Figure 2.2 Curve of sigmoid function versus velocity	7
Figure 2.3 Second-order effect (a) two effects in element (b) sway condition (c) non-sway condition.....	8
Figure 2.4 Framework element (McGuire et al., 1982)	9
Figure 2.5 Pure axial element (a) support system. (b) free-body diagram (McGuire et al., 1982).....	10
Figure 2.6 Beam element (McGuire et al., 1982)	11
Figure 2.7 Deformation of beam element due to applied load (McGuire et al., 1982)	11
Figure 2.8 Transformation of local coordinate to local coordinate.....	13
Figure 3.1 Encoding general solution to BPSO bits	18
Figure 3.2 Flowchart showing the processing of the BPSO algorithm	19
Figure 4.1 Graph of the available bending moment versus width to thickness ratio..	24
Figure 4.2 Graph of the available bending moment versus unbraced length	26
Figure 4.3 Layout of the frame connection	28
Figure 5.1 Benchmark functions with two unknown variables.....	31
Figure 5.2 Curve of minimum fitness versus constant inertia weight.....	33
Figure 5.3 Layout and load of two-bays, three-stories frame	34
Figure 5.4 Strength ratio of elements for two-bays, three-stories frame.....	35

Figure 5.5 Convergence curve for two-bays, three-stories frame.....	36
Figure 5.6 Layout and load of one-bay, ten-stories frame (a) Unbraced frame, (b) Braced frame with original grouping (c) Braced frame with new grouping.....	37
Figure 5.7 Strength Ratio of elements for one-bay, ten-stories frame (No.1).....	38
Figure 5.8 Convergence curve for one-bay, ten-stories frame (No.1).....	39
Figure 5.9 Layout of braced element for minimum weight of one-bay, ten-stories frame (a) Frame No.3 (b) Frame No.4.....	40
Figure 5.10 Layout and strength ratio of elements for one-bay, ten-stories frame (a) frame No.2, (b) frame No.3 and (c) frame No.4.....	42
Figure 5.11 Story drift for one-bay, ten-stories frame (a) frame No.2, (b) frame No.3 and (c) frame No.4.....	43
Figure 5.12 Convergence Curve for one-bay, ten-stories frame (a) frame No.2, (b) frame No.3 and (c) frame No.4.....	44
Figure 5.13 Layout and Load of three-bays, twenty-four-stories unbraced frame.....	46
Figure 5.14 Layout and Load of three-bays, twenty-four-stories braced frame (a) initial grouping (b) new grouping.....	48
Figure 5.15 Layout of braced element for three-bays, twenty-four -stories (a) frame No.2 (b) frame No.3.....	49
Figure 5.16 Story drift for three-bays, twenty-four-stories frame (a) frame No.1, (b) frame No.2 (c) frame No.3.....	52
Figure 5.17 Convergence curve for three-bays, twenty-four-stories frame (a) frame No.1 (b) frame No.2 (c) frame No.3.....	53
Figure 5.18 Element strength ratio for three-bays, twenty-four-stories frame (No.1)..	54
Figure 5.19 Element strength ratio for three-bays, twenty-four-stories frame (No.2)..	54
Figure 5.20 Element strength ratio for three-bays, twenty-four-stories frame (No.3)..	55

Figure 6.1 Two-bay, three-stories frame (a) % optimal found from total runtimes (b) No. of analysis getting minimum weight	56
Figure 6.2 Unbraced one-bay, three-stories frame considering drift at roof (a) minimum weight (b) standard deviation of weight for total runtimes (c) No. of analysis getting minimum weight.....	57
Figure 6.3 Unbraced one-bay, three-stories frame considering drift for all stories (a) minimum weight (b) standard deviation of weight for total runtimes (c) No. of analysis getting minimum weight.....	57
Figure 6.4 minimum weight for all types of one-bay, twenty-four-stories frame.....	58
Figure 6.5 Minimum weight of unbraced frame of three-bay, twenty-four-stories frame.....	58
Figure 6.6 Minimum weight for all types of each three-bay, twenty-four-stories frame	59



CHAPTER 1

INTRODUCTION

1.1 Background

Optimization applies to many industries for reducing the cost of material, labor, and construction. Most optimization problems in real life are large and complex, making solving directly by an exact method is difficult and time-consuming. According to reason, people search for methods to solve these problems in a shorter time. One of these methods is a heuristic technique. A Heuristic is a mathematical technique guaranteeing an optimal point. In some problems, A heuristic technique may trap local optimum that the best solution is best in some regions, but it is not the best solution. A higher level of a heuristic technique called a metaheuristic algorithm technique is developed to solve this problem. The algorithm concept is nature-inspired and using random search with some method to avoid trapping in a local optimum. There are many well-known algorithms such as Genetic Algorithm (GA), Particle swarm optimization (PSO), Binary Particle swarm optimization (BPSO), and Ant colony optimization (ACO).

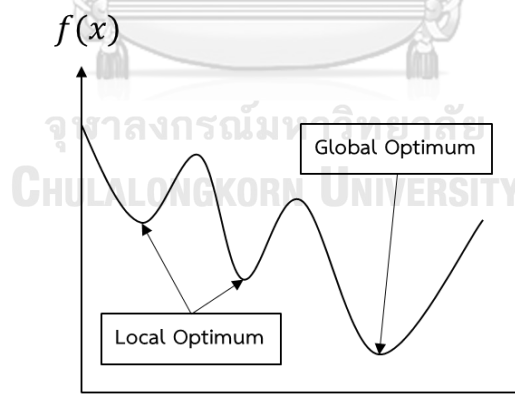


Figure 1.1 Graph indicates local and global optima

Binary Particle Swarm Optimization (BPSO) was developed from Particle Swarm Optimization (PSO) to solve a discrete optimization problem by using a binary system. These algorithms process with the same parameters such as inertia weight, acceleration coefficient, and velocity. Among these parameters, many PSO authors found that inertia weight value significantly influences PSO efficiency. Most PSO

articles used linear decreasing inertia weight from 0.9 to 0.4 for optimization. Due to the same parameters and similar processes, many BPSO authors brought this inertia weight in their article studies. However, they got bad results in their articles.

A meta-heuristic method is a well-known method for solving an optimization problem. In the civil engineering field, most of the optimization problems in real life are structural optimization. The objective of this optimization is to minimize the structural weight to reduce the cost of construction. In the present, many authors study the structural optimization problem by using the different meta-heuristic methods. The benchmark examples they used are unbraced structures. However, the design of the unbraced structure in a high-rise building under lateral load is not efficient. This structural design may lead to significant lateral drift and requires a more extensive cross-sectional area of the structure to carry it. An efficient way to solve this problem is using a bracing system.

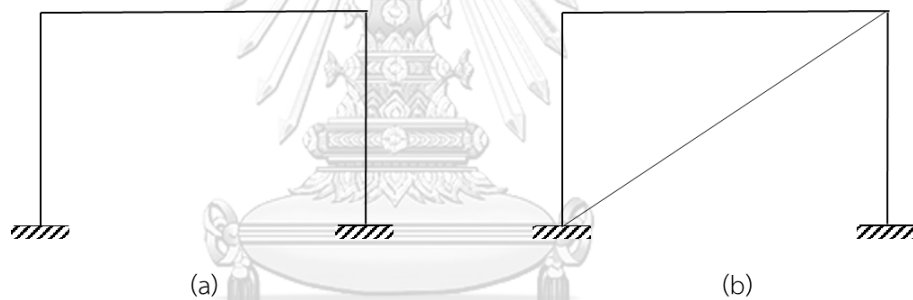


Figure 1.2 Framework (a) unbrace structure (b) braced structure

1.2 Research Objectives

- (1) At present, not many articles studies about the inertia weight of BPSO. Base on applying inertia weight value of PSO in BPSO, many BPSO authors found bad results occurring in their articles. According to this reason, we study varying inertia weight values by aiming to improve the performance of BPSO. The inertia weight samples are studied in mathematical benchmarks and investigated results to find the best inertia weight.
- (2) To compare the efficiency of BPSO with other meta-heuristic algorithms, we apply the best inertia weight from the study in (1) in the structural optimization problems that have more complexity and larger search space. BPSO is studied in weight optimization of the unbraced frame due to varying

cross-sectional areas. The parameters for comparison are the analysis time of convergence, the approach to optimize the solution, and the precision of data when repeated with many numbers of runs.

- (3) Unbrace frame is an ineffective structure to withstand a lateral load. So, the research studies more in the braced frame using X-shape bracing. We compare the minimum weight of the brace frames and unbraced frames using the BPSO algorithm.
- (4) The structural benchmarks for study refer to previous articles that authors classified the elements in groups for decreasing search space. Elements in the same group have the same cross-sectional area. This research studies more about the influence of search space. We classify the original benchmarks of the braced frame to the finer group that increases search space and compare with the initial grouping results.

1.3 Scopes

- (1) The inertia weight samples consist of seven constant inertia weight samples: 0.9, 0.92, 0.94, 0.96, 0.98, 1.00, 1.02, and linear decreasing inertia weight from 0.9 to 0.4. We test the samples on six mathematical benchmark functions.
- (2) We study three planer frame benchmarks using the inertia weight obtained from inertia weight study. The available sections for optimization base on the AISC design section from W6 to W40. We study X-braced frame in only one-bay, ten stories frame and three-bays, twenty-four stories frame.
- (3) The optimization takes place in steel structures. Beam to beam and beam to column connection is assumed to be rigid. In contrast, the X-braced element has pinned end designed to resist only the axial load. We optimize only the cross-sectional area of elements; other properties are constant. In addition, we consider more for the topology optimization of X-brace elements.
- (4) The analysis considers the second-order elastic effects, including $P - \delta$ and $P - \Delta$ effects. The design follows the AISC code considering drift and strength constrained equations, except two-bays, three-stories frame that is considered only the strength constraint equation.

(5) All processes are coded in MATLAB programming.

1.4 Methodology

All processes of frame optimization are coded in MATLAB to search for the solution. The data for coding are follows:

- (1) BPSO algorithm that is the tool for optimization.
- (2) Samples, range of optimization for weight optimization and geometries, material properties, load, and available cross-sectional areas for frame optimization.
- (3) Stiffness analysis, first-order analysis amplification, and design by AISC code for frame optimization.
- (4) The objective function and constrained functions.
- (5) An expected result that we need from the study.

For the BPSO process, available solutions or a cross-sectional area of elements must be transformed into binary space by encoding solutions in real numbers into BPSO binary bits. The algorithm is run until it reaches to stopping criteria.

CHAPTER 2

LITERATURE REVIEW

2.1 Binary Particle Swarm Optimization (BPSO)

2.1.1 Background of BPSO

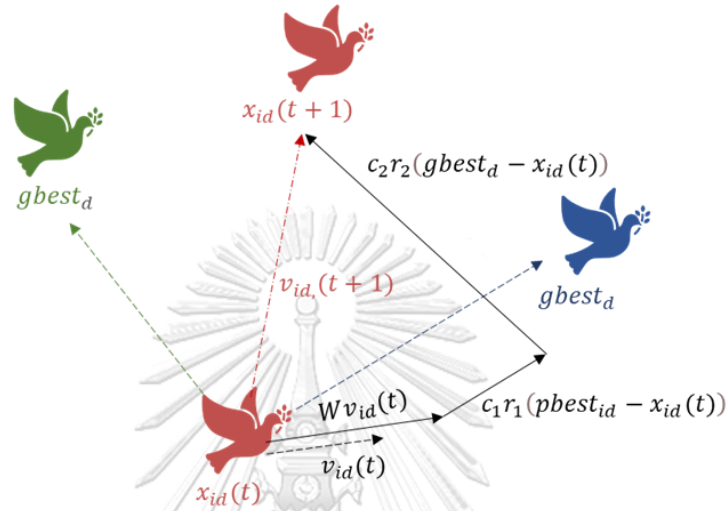


Figure 2.1 Updating PSO particle

The binary particle swarm optimization algorithm (BPSO) proposed by (Kennedy & Eberhart, 1997) is a discrete version of the particle swarm optimization algorithm (PSO) by (Eberhart & Kennedy, 1995). The movement of animals inspires these algorithms, like bird flocks for searching the food. All birds move towards the food that one can find and get closer to the food when time past. PSO technique assumes each bird as a particle, the flock as a population, and food as the best solution. Each particle has the position and velocity of itself changed by iteration. Particle memorizes the position giving the best solution until now of itself as *pbest* and population as *gbest*. The updates of position and velocity are in Eq. (2.1), (2.2). It should be noted that the number of dimensions equals the number of unknown variables in the problem.

$$v_{id,t+1} = v_{id,t} + c_1 r_1 (pbest_{id} - x_{id,t}) + c_2 r_2 (gbest_d - x_{id,t}) \quad (2.1)$$

$$x_{id,t+1} = x_{id,t} + v_{id,t+1} \quad (2.2)$$

Where $v_{id,t}$ and $x_{id,t}$ = velocity and position of particle i in dimension d by iteration t , respectively

c_1 = cognitive coefficient usually taken as 2.0

c_2 = social coefficient usually taken as 2.0

r_1 and r_2 = random number between 0 and 1 for PSO and a random number of 0 and 1 for BPSO

$pbest_{id}$ = individual best position of particle i in dimension d

$gbest_d$ = population best position in dimension d

Eq. (2.1) consists of three parts. The first is the velocity part. The second and the third parts specify the update of new velocity decided by how far of the position from $pbest$ and $gbest$. The first part adjusts how far explosion particle searches in search space. So, the global search specifies in this part. The second and the third part indicate the direction of particle search approach the best solution. These parts specify the local search. To balance the ability of local search and global search, (Shi & Eberhart, 1998) modified Eq. (2.1) by adding inertia weight W to the first part as in Eq. (2.3). This equation is an equation many researchers used to study PSO instead of Eq. (2.1).

$$v_{id,t+1} = Wv_{id,t} + c_1r_1(pbest_{id,t} - x_{id,t}) + c_2r_2(gbest_{d,t} - x_{id,t}) \quad (2.3)$$

BPSO works on the concept of a particle moving in binary space by bit-string. One bit has only two available solutions, which are 0 and 1. According to the binary concept, we need many bits to fill all available solutions of each unknown variable. When the total bit is equal to n bit, all available solutions are 2^n . For example, the total bits for available solutions of four are two bits. The available solutions in the form of a bit are "00", "01", "10" and "11". For movement of a particle in binary space, the update of position in Eq. (2.2) is changed to be dependent on the relationship between random numbers from 0 to 1 or r and sigmoid function of particle's velocity $S(v_{id})$ as Eq. (2.4) and (2.5). It should be noted that the number of dimensions d in Eq. (2.4) and Eq. (2.5) equals the number of total bits used in the problem.

$$S(v_{id}) = Sigmoid(v_{id}) = \frac{1}{1 + e^{-v_{id}}} \quad (2.4)$$

$$\begin{aligned} \text{if } r < S(v_{id,t+1}) \text{ then } x_{id,t+1} &= 1 \\ \text{else } x_{id,t+1} &= 0 \end{aligned} \quad (2.5)$$

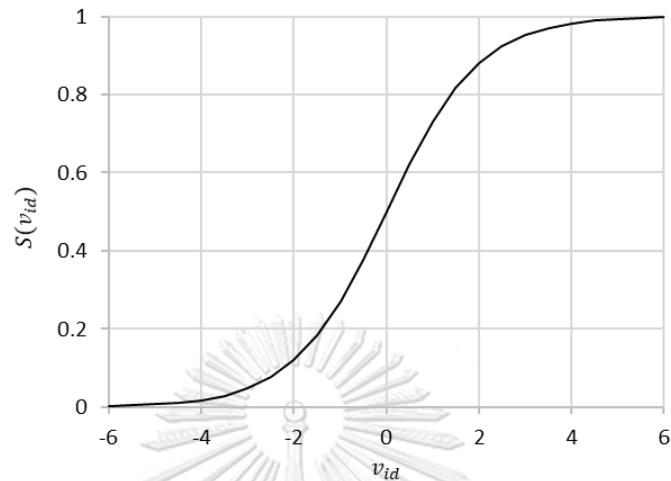


Figure 2.2 Curve of sigmoid function versus velocity

2.1.2 Previous PSO Articles on Inertia Weight

Besides modifying the updating velocity equation as Eq. (2.3), (Shi & Eberhart, 1998) studied varying inertia weight. They used constant inertia weight and time-varying inertia weight as their experiment simple. The constant inertia weight value they selected is 0, 0.8, 0.85, 0.9, 0.95, 1, 1.05, 1.1, 1.2, and 1.4. The time-varying inertia weight is the linear decreasing inertia weight from 1.4 to 0. They tested these values on Schaffer's f_6 function. The experiment results show that the constant inertia weights in the range [0.9,1.2] gave a good result on average. They also suggested the future research try the linear decreasing in different values. From Eq. (2.3), many PSO researchers recommended the linear decreasing inertia weight from 0.9 to 0.4 to be the inertia weight giving the best result (Poli, Kennedy, & Blackwell, 2007).

2.1.3 Previous BPSO Articles

According to the same parameters between PSO and BPSO, most BPSO articles refer to PSO articles. However, some parameters giving good performance in the PSO algorithm did not work well in the BPSO algorithm. According to this reason, the authors studied improving BPSO performance. The examples of improving BPSO are using the new function to replace the sigmoid function (Mirjalili & Lewis, 2013) and

(Guo, Wang, & Guo, 2020) and using a hybrid version of BPSO combine with another algorithm (Mirjalili, Wang, & Coelho, 2014).

2.2 Structural Analysis

2.2.1 General

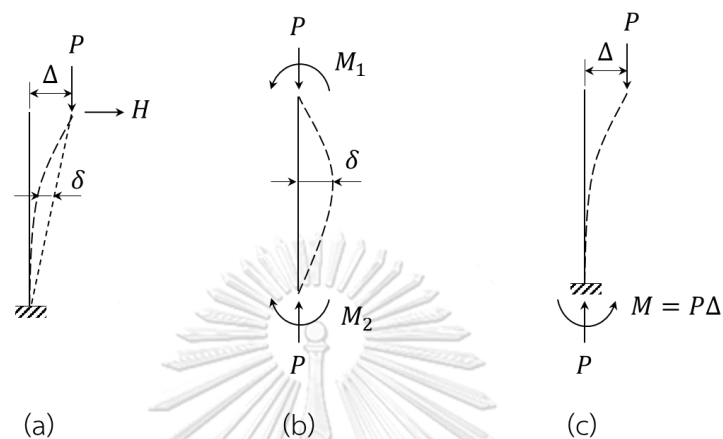


Figure 2.3 Second-order effect (a) two effects in element (b) sway condition (c) non-sway condition

The first order elastic is about the deformation from the applied load. When the structure is deformed due to applied load, it causes some eccentricity, as shown in *Figure 2.3*. When the element has a sway condition, it moves laterally from its original position due to applied load, especially lateral load. The displacement structure moves from its original position called Δ . This eccentricity leads to additional moments due to $P - \Delta$ effect. When element is under non-sway condition, it causes delta due to buckling called $P - \delta$. From considering these two effects, the analysis is called second-order elastic analysis.

The stiffness method is one of the popular methods used for structural analysis. However, the stiffness method is ineffective when the second-order effect, like the P-delta and P-delta, are interested. This method is time-consuming due to having an iteration process for the geometric stiffness part. The amplified first-order method by AISC is replaced for analysis of second-order structural problems.

2.2.2 Stiffness Matrix Analysis

The stiffness matrix analysis (McGuire, Gallagher, & Saunders, 1982) is the concept of finding unknown displacement from the known force. From *Figure 2.4*, there are

12 degrees of freedom of the 3D element. However, the planer frame considering only two-axis reduces the degree of freedom reduce into 6 degrees of freedom which are $F_{x1}, F_{x2}, M_{z1}, F_{y2}, F_{y2}$ and M_{z2} .

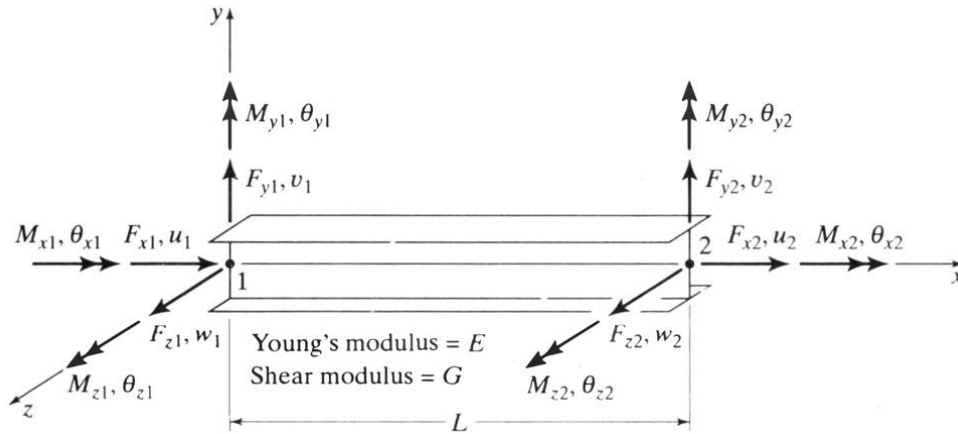


Figure 2.4 Framework element (McGuire et al., 1982)

Maxwell's reciprocal theorem, or a special case of Betti's law, said that the displacements at point 1 correspond to the unit load at point 2 is the same as the displacements at point 2 correspond to the unit load at point 1 as Eq. (2.6).

$$\Delta_{12}P_1 = \Delta_{21}P_2 \quad (2.6)$$

From Maxwell's reciprocal theorem, the stiffness matrix k that is described the relationship of force F and displacement Δ as Eq. (2.7) can be $k_{ij} = k_{ji}$

$$\begin{Bmatrix} F_f \\ F_s \end{Bmatrix} = \begin{bmatrix} k_{ff} & k_{fs} \\ k_{sf} & k_{ss} \end{bmatrix} \begin{Bmatrix} \Delta_f \\ \Delta_s \end{Bmatrix} \quad (2.7)$$

Where f = free degree of freedom

s = support degree of freedom

Where the displacement at support degree of freedom is equal to 0, Eq. (2.7) can be written as Eq. (2.8).

$$\begin{Bmatrix} F_f \\ F_s \end{Bmatrix} = \begin{bmatrix} k_{ff} \\ k_{sf} \end{bmatrix} \{\Delta_f\}; \{F_f\} = [k_{ff}]\{\Delta_f\} \quad (2.8)$$

The reaction force is equal to the action force from the equilibrium system as Eq. (2.9).

$$\{F_s\} = [\Phi]\{F_f\} \quad (2.9)$$

$$\{F_s\} = [\Phi][k_{ff}]\{\Delta_f\} \quad (2.10)$$

$$\{F_s\} = [k_{sf}]\{\Delta_f\}; [k_{sf}] = [\Phi][k_{ff}] \quad (2.11)$$

Correspond to the symmetry property, $[k_{fs}]$ can be explained as Eq. (2.12)

$$[k_{fs}] = [k_{sf}]^T = [k_{ff}] [\Phi]^T \quad (2.12)$$

When $\{F_s\} = [\Phi]\{F_f\}$ as Eq. (2.9), Eq. (2.7) is also explained as the bottom part is equal to $[\Phi]$ multiply by top part as Eq. (2.13).

$$\{k_{ss}\} = [\Phi]\{k_{fs}\} = [\Phi][k_{ff}] [\Phi]^T \quad (2.13)$$

$$[k] = \begin{bmatrix} [k_{ff}] & [k_{ff}] [\Phi]^T \\ [\Phi][k_{ff}] & [\Phi][k_{ff}] [\Phi]^T \end{bmatrix} \quad (2.14)$$

$$\{k_{ss}\} = [\Phi]\{k_{fs}\} = [\Phi][k_{ff}] [\Phi]^T \quad (2.15)$$

For axial deformation of the element with support in Fig. (2.5a), a relationship between stress and strain is derived as Eq. (2.6).

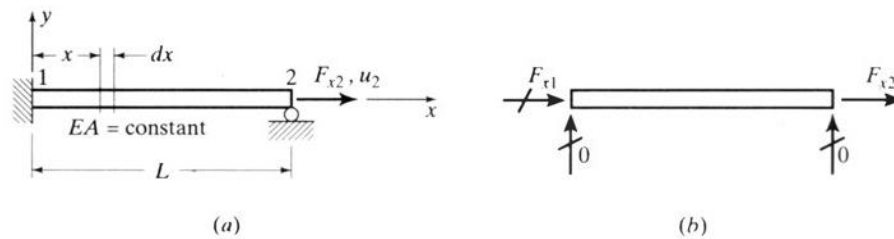


Figure 2.5 Pure axial element (a) support system, (b) free-body diagram (McGuire et al., 1982)

$$u_2 = \int_0^L e \, dx = \int_0^L \frac{\sigma}{E} \, dx = \int_0^L \frac{F_{x2}}{EA} \, dx = \frac{F_{x2}L}{EA} \quad (2.16)$$

$$F_{x2} = \frac{EA}{L} u_2 = k_{22} u_2 \quad (2.17)$$

From the equilibrium equation, Eq. (2.18) can be explained as follows.

$$F_{x1} = (-1)F_{x2}; [\Phi] = -1 \quad (1.18)$$

When we substitute Eq. (2.11), (2.12), (2.15), and (2.18) to Eq. (2.7), the equation can be written as follows.

$$\begin{Bmatrix} F_{x1} \\ F_{x2} \end{Bmatrix} = \frac{EA}{L} \begin{bmatrix} 1 & -1 \\ -1 & 1 \end{bmatrix} \begin{Bmatrix} u_1 \\ u_2 \end{Bmatrix} \quad (2.19)$$

The beam element from Figure (2.6) can be explained the relationship between stress and strain as Eq. (2.20).

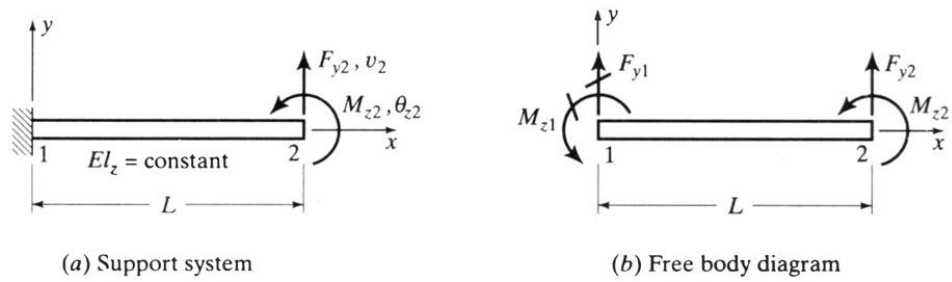


Figure 2.6 Beam element (McGuire et al., 1982)

$$e_x = \frac{-y}{\rho} = -y \frac{d^2 v}{dx^2} \quad (2.20)$$

Where ρ radius of curvature. $\sigma_x = E e_x$

$$\sigma_x = -E y \frac{d^2 v}{dx^2} \quad (2.21)$$

$$M_z = \int_A E \frac{d^2 v}{dx^2} y^2 dA = EI_z \frac{d^2 v}{dx^2} \quad (2.22)$$

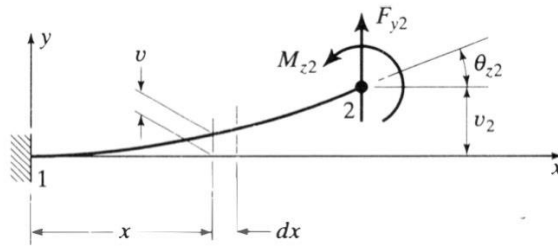


Figure 2.7 Deformation of beam element due to applied load (McGuire et al., 1982)

From Figure 2.7, moment equation $M_z(x)$ can be written as Eq. (2.23)

$$\frac{d^2 v(x)}{dx^2} = \frac{M_z(x)}{EI_z} = \frac{F_{y2}(L-x) + M_{z2}}{EI_z} \quad (2.23)$$

From Integrating Eq. (2.23), the new equations are in Eq. (2.24) and (2.25).

$$\frac{dv(x)}{dx} = \theta_z(x) = \frac{1}{EI_z} \left[F_{y2} \left(\frac{Lx^2}{2} - \frac{x^3}{6} \right) + \frac{M_{z2}x^2}{2} \right] + C_1x + C_2 \quad (2.24)$$

$$v(x) = \frac{1}{EI_z} \left[F_{y2} \left(\frac{Lx^2}{2} - \frac{x^3}{6} \right) + \frac{M_{z2}x^2}{2} \right] + C_1x + C_2 \quad (2.25)$$

From Boundary Condition, $\theta(0) = 0$ and $v(0) = 0$, we get $C_1 = 0$ and $C_2 = 0$. Eq. (2.24) and (2.25) can be written at position $x = L$ as Eq. (2.26) and (2.27), respectively.

$$v_2 = v(L) = \frac{F_{y2}L^3}{3EI_z} + \frac{M_{z2}L^3}{2EI_z} \quad (2.26)$$

$$\theta_{z2} = v(L) = \frac{F_{y2}L^2}{2EI_z} + \frac{M_{z2}L}{EI_z} \quad (2.27)$$

Eq. (2.26) and (2.27) can be written in matrix form as Eq. (2.28) and (2.29)

$$\begin{Bmatrix} v_2 \\ \theta_{z2} \end{Bmatrix} = \frac{L}{EI_z} \begin{bmatrix} \frac{L^2}{3} & \frac{L}{2} \\ \frac{L}{2} & 1 \end{bmatrix} \begin{Bmatrix} F_{y2} \\ M_{z2} \end{Bmatrix} \quad (2.28)$$

$$\begin{Bmatrix} F_{y2} \\ M_{z2} \end{Bmatrix} = \frac{EI_z}{L} \begin{bmatrix} \frac{12}{L^2} & -\frac{6}{L} \\ -\frac{6}{L} & 4 \end{bmatrix} \begin{Bmatrix} v_2 \\ \theta_{z2} \end{Bmatrix} \quad (2.29)$$

From equilibrium equations as Eq. (2.30) and (2.31), They can be written into matrix form as Eq. (2.32).

$$F_{y1} = -F_{y2} \quad (2.30)$$

$$M_{z1} = -F_{y2}L - M_{z2} \quad (2.31)$$

$$\begin{Bmatrix} F_{y1} \\ M_{z1} \end{Bmatrix} = \frac{EI_z}{L} \begin{bmatrix} -1 & 0 \\ -L & -1 \end{bmatrix} \begin{Bmatrix} F_{y2} \\ M_{z2} \end{Bmatrix} \quad (2.32)$$

When we substitute Eq. (2.11), (2.12), (2.15), and (2.32) to Eq. (2.7), the equation can be written as follows:

$$\begin{Bmatrix} F_{y1} \\ M_{z1} \\ F_{y2} \\ M_{z2} \end{Bmatrix} = \begin{bmatrix} \frac{12EI}{L^3} & \frac{6EI}{L^2} & -\frac{12EI}{L^3} & \frac{6EI}{L^2} \\ \frac{6EI}{L^2} & \frac{4EI}{L} & -\frac{6EI}{L^2} & \frac{2EI}{L} \\ \frac{12EI}{L^3} & -\frac{6EI}{L^2} & \frac{12EI}{L^3} & -\frac{6EI}{L^2} \\ -\frac{6EI}{L^2} & \frac{2EI}{L} & \frac{6EI}{L^2} & \frac{4EI}{L} \end{bmatrix} \begin{Bmatrix} v_1 \\ \theta_{z1} \\ v_2 \\ \theta_{z2} \end{Bmatrix} \quad (2.33)$$

Eq. (2.19) and (2.33) can be an assembly for six degrees of freedom matrix as Eq. (2.34).

$$\begin{Bmatrix} F_{x1} \\ F_{y1} \\ M_{z1} \\ F_{x2} \\ F_{y2} \\ M_{z2} \end{Bmatrix} = \begin{bmatrix} \frac{AE}{L} & 0 & 0 & -\frac{AE}{L} & 0 & 0 \\ 0 & \frac{12EI}{L^3} & \frac{6EI}{L^2} & 0 & -\frac{12EI}{L^3} & \frac{6EI}{L^2} \\ 0 & \frac{6EI}{L^2} & \frac{4EI}{L} & 0 & -\frac{6EI}{L^2} & \frac{2EI}{L} \\ -\frac{AE}{L} & 0 & 0 & \frac{AE}{L} & 0 & 0 \\ 0 & -\frac{12EI}{L^3} & -\frac{6EI}{L^2} & 0 & \frac{12EI}{L^3} & -\frac{6EI}{L^2} \\ 0 & \frac{6EI}{L^2} & \frac{2EI}{L} & 0 & -\frac{6EI}{L^2} & \frac{4EI}{L} \end{bmatrix} \begin{Bmatrix} u_1 \\ v_1 \\ \theta_{z1} \\ u_2 \\ v_2 \\ \theta_{z2} \end{Bmatrix} \quad (2.34)$$

All equations above describe the degree of freedom in the local coordinate system. The transformation matrix is used to transform the local coordinate system into a global coordinate system. From the equilibrium equation, the local coordinate can be converted to global coordinate as following equations.

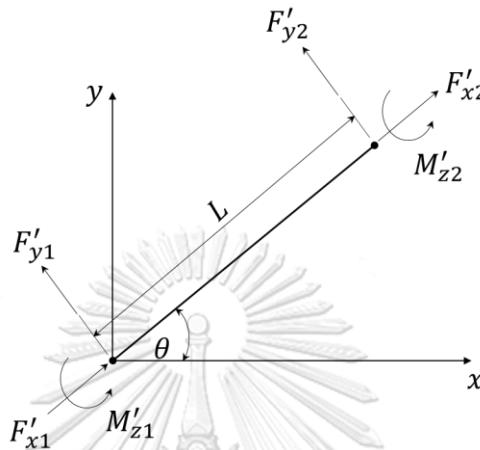


Figure 2.8 Transformation of local coordinate to local coordinate

$$F_x = F'_x \cos\theta - F'_y \sin\theta \quad (2.35)$$

$$F_y = F'_x \sin\theta + F'_y \cos\theta \quad (2.36)$$

$$M_z = M'_z \quad (2.37)$$

$$\begin{Bmatrix} F_{x1} \\ F_{y1} \\ M_{z1} \\ F_{x2} \\ F_{y2} \\ M_{z2} \end{Bmatrix} = \begin{bmatrix} \cos\theta & -\sin\theta & 0 & 0 & 0 & 0 \\ \sin\theta & \cos\theta & 0 & 0 & 0 & 0 \\ 0 & 0 & 1 & 0 & 0 & 0 \\ 0 & 0 & 0 & \cos\theta & -\sin\theta & 0 \\ 0 & 0 & 0 & \sin\theta & \cos\theta & 0 \\ 0 & 0 & 0 & 0 & 0 & 1 \end{bmatrix} \begin{Bmatrix} F'_{x1} \\ F'_{y1} \\ M'_{z1} \\ F'_{x2} \\ F'_{y2} \\ M'_{z2} \end{Bmatrix} \quad (2.38)$$

$$\{F\} = [T]\{F'\} \quad (2.39)$$

$$\{F\} = [T][K']\{U'\} = [T][K'] [T]\{U\} \quad (2.40)$$

$$[K] = [T][K'] [T] \quad (2.41)$$

2.2.3 Amplified First-Order Elastic Analysis by AISC

The method is approximate to calculate second-order analysis from the first-order analysis (AISC, 2016). We need to analyze the first-order analysis of the structure for two situations: frame in non-sway condition and frame in sway condition. The first-order analysis for the non-sway condition is amplified by moment amplification factor due to $P - \Delta$ effect B_1 . The first-order analysis for the sway condition is amplified by moment amplification factor due to $P - \delta$ effect B_2 as Eq. (2.42) and

(2.43).

$$P_r = P_{nt} + B_2 P_{lt} \quad (2.42)$$

$$M_r = B_1 M_{nt} + B_2 M_{lt} \quad (2.43)$$

Where P_{nt} and M_{nt} = required first-order axial strength and bending moment with no sway condition, respectively

P_{lt} and M_{lt} = required first-order axial strength and bending moment with sway condition, respectively

B_1 = moment amplification factor due to $P - \Delta$ effect calculated from Eq. (2.44)

B_2 = moment amplification factor due to $P - \delta$ effect calculated from Eq. (2.45)

$$B_1 = \frac{C_m}{1 - \frac{P_u}{P_{e1}}} \quad (2.44)$$

Where C_m = moment gradient coefficient assuming no translation calculated from moment at the ends of the element where $M_1 \leq M_2$ as shown in Eq. (1.45)

P_u = the first-order axial strength

P_{e1} = elastic critical buckling of the element with no sway condition

$$C_m = 0.6 - 0.4 \frac{M_1}{M_2} \quad (2.45)$$

$$B_2 = \frac{1}{1 - \frac{P_{story}}{\sum P_{e2}}} \quad (2.46)$$

Where P_{story} = total vertical loads

$\sum P_{e2}$ = elastic critical buckling strength for the story with sway condition

2.3 Unbraced Frame VS Braced Frame Design against Lateral Load

An unbraced frame is also known as a moment-resisting frame consisting of two types of elements: beam and column. Column and beam elements connect perpendicularly with a rigid joint. The moment resisting frame only can withstand the vertical load. However, this structure is sensitive to lateral loads such as seismic

loads and wind loads. High-rise moment-resisting structures under lateral load may cause a significant drift that leads to a lack of serviceability function. The structure cross-section area needs to design a huge size to avoid drift. It consumes too much material to construct, which leads to uneconomical design.

A braced frame is a well-known structure design to resist the lateral load. This structure has a bracing system that the tools to reduce lateral drift of structure. The bracing system can be from many shapes such as X-shape, V-shape, and K-shape. Many research experiments confirm that brace frames can reduce the lateral drift, such as (Haque, Atik, Muhtadi, & Zasiah) and (Jagadish & Doshi, 2013)

2.4 Steel Structural Optimization using Meta-heuristic Algorithm

Many authors studied on moment-resisting planar frame optimization problem using meta-heuristic algorithms such as GA (Pezeshk, Camp, & Chen, 2000), ACO (Camp, Bichon, & Stovall, 2005), TLBO (Toğan, 2012), and SBO (Farshchin, Maniat, Camp, & Pezeshk, 2018). They apply algorithms in the unbraced structure under vertical and lateral load applied on the structure. The design of structures was under the AISC specification for strength and lateral drift design considering the second-order effect ($P - \Delta$ and $P - \delta$ effects). However, the design for stability by AISC specification isn't only considering second-order effect. The specification includes other requirements such as geometric imperfections, stiffness reductions due to inelasticity. ESO (Chaiwongnoi, Van Thu, Tangaramvong, & Van, 2020) is research considered the design for stability using the direct analysis method by AISC specification.

CHAPTER 3

BINARY PARTICLE SWARM OPTIMIZATION ALGORITHM

3.1 General

According to the introduction of the BPSO algorithm in section 2.1, this chapter specifies more detail about the algorithm. The detail includes the process of the algorithm in step by step, selecting BPSO parameters, and encoding real number value into binary code.

3.2 BPSO Parameters

Selecting parameters has much influence on the BPSO algorithm. It can upgrade or downgrade the performance of the algorithm significantly. The parameters set up in this research are as follows.

3.2.1 Initial Parameters

There are two parameters, velocity and position of particles, are set as the initial parameters. This research decides to select the initial parameters randomly. The reason behind this decision is to govern as much as the possibility of searching for the solution. The initial position is generated with binary values 0 and 1. Initial velocity is generated randomly in the range of $[-v_{max}, v_{max}]$. The formulations to random initial position and velocity are in Eq. (3.1) and Eq. (3.2), respectively.

$$\text{if } rand_{id} < 0.5 \text{ then } x_{id} = 1 \\ \text{else } x_{id} = 0 \quad (3.1)$$

$$v_{id} = -v_{max} + rand * 2v_{max} \quad (3.2)$$

Where x_{id} = position of particle i at d dimension

v_{id} = velocity of particle i at d dimension

v_{max} = Maximum velocity usually equal to 6 that is the range of sigmoid curve of sigmoid function versus velocity

$rand$ = random number from 0 to 1

3.2.2 Inertia Weight

(Shi & Eberhart, 1998) found the constant inertia weight in the range of [0.9, 1.2], giving the best solution in average among their samples. Besides, the result from PSO research (Poli et al., 2007) found linear decreasing inertia weight from 0.9 to 0.4 gave

high efficiency to the algorithm. In this BPSO research, we study on constant inertia weight 0.9, 0.92, 0.94, 0.96, 0.98, 1.00, 1.02 referring to (Shi & Eberhart, 1998) and linear decreasing inertia weight from 0.9 to 0.4 referring to (Poli et al., 2007).

$$W_c(t) = W_c \quad (3.3)$$

$$W_{LD}(t) = W_{max} - \frac{W_{max} - W_{min}}{t_{max}} t \quad (3.4)$$

Where W_c = Constant Inertia weight

W_{LD} = Linear Decreasing Inertia Weight at iteration

W_{max} = Maximum inertia weight

W_{min} = Minimum inertia weight

t = iteration

t_{max} = Maximum iteration

3.2.3 Stopping Criteria

BPSO algorithm requires repeating the loop many times to reach the optimal solution. The loop continues with a continuous process if it doesn't have a stop criteria. So, we must define the maximum iteration to stop the process. We should select the suitable maximum iteration that can show solution convergence by not using too long a loop. BPSO algorithm deals with a population of particles that all have a relationship with others, so the BPSO loop in each iteration can finish only when we evaluate all particles. So, the stopping criteria are satisfied if an iteration reaches the maximum iteration, and all particles are considered as *Figure 3.2*

3.3 The Transformation between Binary Space and Real Number Space

Sometimes, the number of positions in real number space is not equal to the number of positions in binary space. Binary space can carry only two available solutions, as explained in section 2.1.1, so it is necessary to add more bits if the binary system takes more possible solutions, as shown in *Figure 3.1*.

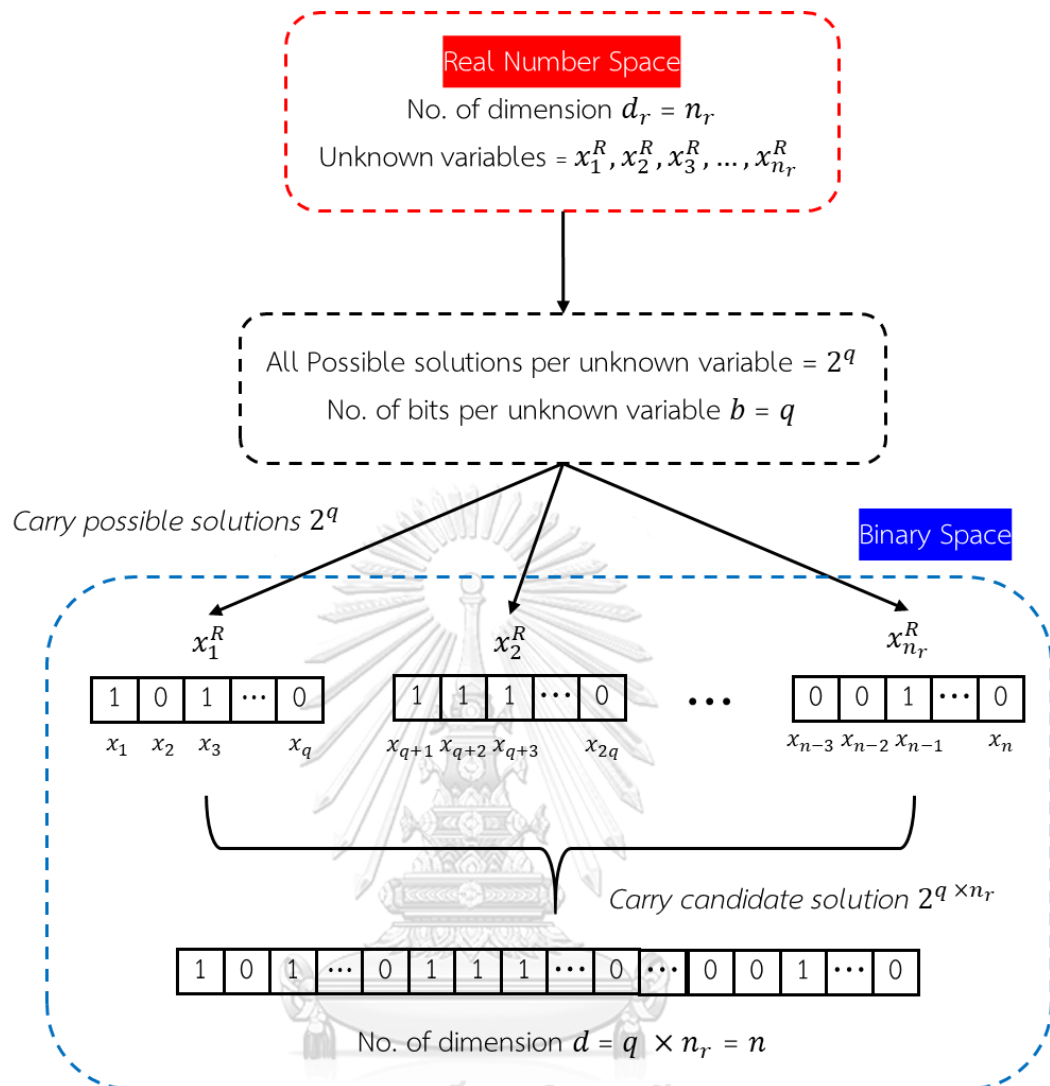


Figure 3.1 Encoding general solution to BPSO bits

To calculate the fitness of objective function $f(x)$, positions of the particle or unknown variables x in binary space are necessary to decode to real number space. The transformation is explained in Eq. (3.6). The values converted by using this equation can be formed only as an integer.

$$x = x_1, x_2, x_3, \dots, x_q \tag{3.5}$$

$$x^R = 1 + 2^0 x_1 + 2^1 x_2 + \dots + 2^{q-1} x_q \tag{3.6}$$

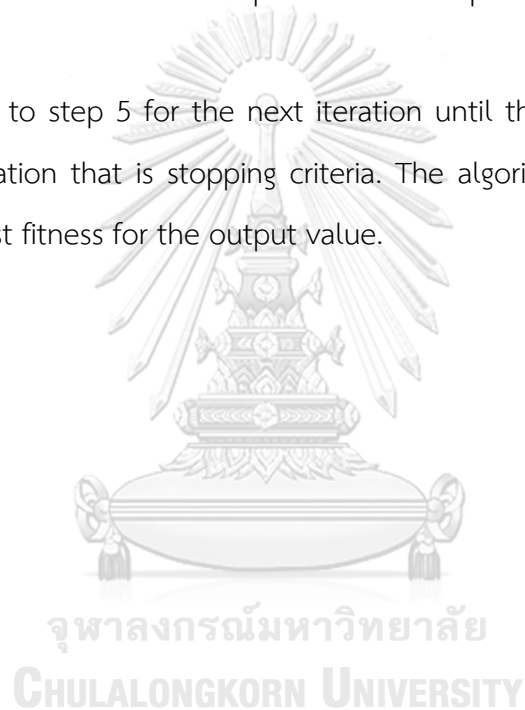
Where x = Positions of the particle in binary space

x^R = position of the particle in real number space

q = No. of bit for one unknown variable

become x_{id} . G-best variables are updated if $fitness_i$ is less than $fitness_gbest$. $fitness_gbest$ is become $fitness_i$, and $gbest_d$ is become x_{id} .

- 4) Update velocity and position of each dimension as Eq. (1.3), (1.4) and (1.5). The updated velocities are restricted not to exceed $[-v_{max}, v_{max}]$. The velocity is $-v_{max}$ if it is less than $-v_{max}$. On the other hand, velocity is v_{max} if it is greater than v_{max} .
- 5) After velocity and position are updated for all dimensions of the particle, the next particle is done in the same process from step 2 to step 4 until all particles are done.
- 6) Repeat step 2 to step 5 for the next iteration until the iteration is reached the maximum iteration that is stopping criteria. The algorithm is done working, and we get the best fitness for the output value.



CHAPTER 4

STRUCTURAL OPTIMIZATION

4.1 General

We study on optimization of steel frame structures under various applied loads. Two types of frames: the moment-resisting frame and X-braced frame, are studied to minimize their weight.

4.2 Objective and Constrained Functions

The objective of this optimization is to minimize the weight of the whole structure, so the objective function is the sum of the weight of all elements shown in Eq. (4.1).

$$\text{minimize } W = \sum_{i=1}^{N_e} W_i L_i \quad (4.1)$$

Where W = the weight of the whole structure

W_i and L_i = cross-sectional weight and length of element i , respectively

N_e = number of total elements.

We design the structures with limitations of strength and story drift. These values shall not exceed the allowable value following the AISC-LRFD code (AISC, 2016). The relationship between demand and allowable value of story drift and strength is in Eq. (4.2) and (4.3).

$$\alpha_{d,i} = \frac{|\Delta_i|}{|\Delta_i^a|} - 1 \leq 0 \quad (4.2)$$

$$\alpha_{I,j} = |\sigma_j| - 1 \leq 0 \quad (4.3)$$

Where $\alpha_{d,i}$ = drift constrained function

Δ_i and Δ_i^a = drift from analysis and allowable drift

$\alpha_{I,j}$ = interaction equation constrained function

σ_j = interaction equation following AISC code

Because the BPSO algorithm cannot handle constrained problems, we must transform the above problem into unconstrained problems. The penalty method (Feiring, Phillips, & Hogg, 1985) is selected to deal with this situation. The concept of the penalty method is adding some penalty value to the objective function when

some constrained function is violated. In this problem, the objective function Eq. (4.1), (4.2), and (4.3) can be revised as follows.

$$\text{minimize } \varphi = W(1 + cP)^\varepsilon \quad (4.4)$$

$$P = \sum_{i=1}^{Ns} \max(\alpha_{d,i}, 0) + \sum_{j=1}^{Ne} \max(\alpha_{l,j}, 0) \quad (4.5)$$

Where φ = new objective function in form of unconstrained function

c and ε = penalty coefficient

P = penalty equation

Ns = number of total stories

Ne = number of total elements.

4.3 AISC-LRFD Design

4.3.1 Story Drift Design

Base on AISC, the inter-story drift limit varies usage from $\frac{h}{100}$ to $\frac{h}{600}$ depending on structure type and cladding type or partition material. However, the most widely used are $\frac{h}{400}$ to $\frac{h}{500}$. The inter-story drift on this research follows the previous research that studies structural optimization. They used inter-story drift equal to $\frac{h}{300}$.

4.3.2 Strength Design

AISC-LRFD code provides the equation for combining axial and bending moment equation called "Interaction equations" as follows.

$$\sigma_j = \frac{P_r}{2\phi_c P_n} + \frac{M_r}{\phi_b M_n} \quad \text{if} \quad \frac{P_u}{\phi_c P_n} < 0.2 \quad (4.6)$$

$$\sigma_j = \frac{P_r}{\phi_c P_n} + \frac{8}{9} \frac{M_r}{\phi_b M_n} \quad \text{if} \quad \frac{P_u}{\phi_c P_n} \geq 0.2 \quad (4.7)$$

Where P_r and P_n = required and available axial strength, respectively

M_r and M_n = required and available bending moment, respectively

ϕ_c and ϕ_b = safety factor of axial strength and bending moment

4.3.2.1 Axial Strength Design

The element under axial load is classified into two types of elements:

compression element and tension element. This research assumes not to consider the effect of connection, so available axial strength for tension element is considered only yielding failure. Available axial strength can be determined as Eq. (4.8) for compression element and Eq. (4.9) for tension element.

$$P_n = A_g F_y \quad (4.8)$$

$$P_n = A_g F_{cr} \quad (4.9)$$

Where A_g = cross-sectional area

F_y = yield strength

F_{cr} = critical buckling stress calculated as Eq. (13) and (14).

$$F_{cr} = F_y 0.658 \frac{F_y}{F_e} \quad \text{if} \quad \frac{KL}{r} \leq 4.71 \sqrt{\frac{E}{F_y}} \quad (4.10)$$

$$F_{cr} = 0.877 F_e \quad \text{if} \quad \frac{KL}{r} > 4.71 \sqrt{\frac{E}{F_y}} \quad (4.11)$$

$$F_e = \frac{\pi^2 E}{\left(\frac{KL}{r}\right)^2} \quad (4.12)$$

Where F_e = Euler buckling stress

E = Young's modulus

K = effective length factor can be calculated from Eq. (4.13) for unbraced frame and Eq. (4.14) for braced frame.

L and r = length and radius of gyration of element, respectively.

$$K_{unb} = \sqrt{\frac{1.6G_A G_B + 4(G_A + G_B) + 7.5}{G_A + G_B + 7.5}} \quad (4.13)$$

$$K_b = \frac{3G_A G_B + 1.4(G_A + G_B) + 0.64}{3G_A G_B + 2(G_A + G_B) + 1.28} \quad (4.14)$$

Where G_A and G_B = beam-column ratio at the ends of the column shows in Eq. (4.15)

$$G = \frac{\Sigma(I/L)_{column}}{\Sigma(I/L)_{beam}} \quad (4.15)$$

4.3.2.2 Flexural Strength Design

According to the AISC code, available bending moments of different element section types are calculated differently because of different behavior. So, the first step for finding available bending moments is to categorize element types. All optimized sections in this research are W-section. The equations for calculating flexural strength are focused only on I-section. Element categories can be defined from the width to thickness ratio of the element, as shown in *Figure 4.2* and Eq. (4.16) to (4.18).

if $\lambda \leq \lambda_p$ then Compact section (4.16)

elseif $\lambda_p < \lambda \leq \lambda_r$ then Non-compact section (4.17)

else Slender section (4.18)

Where λ = width to thickness ratio of the element as Eq. (4.19) and (4.20)

λ_p = Limit of width to thickness ratio for compact section as Eq. (4.21) and (4.22)

λ_r = Limit of width to thickness ratio for non-compact section as Eq. (4.23) and (4.24)

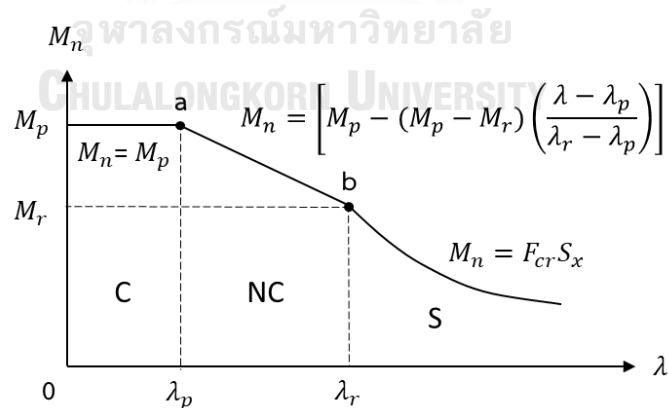


Figure 4.1 Graph of the available bending moment versus width to thickness ratio

$$\lambda_f = \frac{b_f}{2t_f} \quad (4.19)$$

$$\lambda_w = \frac{h}{t_w} \quad (4.20)$$

Where λ_f = width to thickness ratio of flange

b_f = width of flange

t_f = thickness of flange

λ_w = width to thickness ratio of web

h = height of section

t_w = thickness of web

$$\lambda_{pf} = 0.38 \sqrt{\frac{E}{F_y}} \quad (4.21)$$

$$\lambda_{pw} = 3.76 \sqrt{\frac{E}{F_y}} \quad (4.22)$$

Where λ_{pf} = limiting width to thickness ratio for compact flange of W-section

λ_{pw} = limiting width to thickness ratio for compact web of W-section

$$\lambda_{rf} = 1.0 \sqrt{\frac{E}{F_y}} \quad (4.23)$$

$$\lambda_{rw} = 5.70 \sqrt{\frac{E}{F_y}} \quad (4.24)$$

Where λ_{rf} = limiting width to thickness ratio for non-compact flange of W-section

λ_{rw} = limiting width to thickness ratio for non-compact web of W-section

Considering properties of available sections from section 4.4.2. and unbraced length from section 5.3., the sections are classified only as compact web sections with compact and non-compact web sections. So, there are two cases to consider: compact web and flange section case and compact web and non-compact flange section case shown in *Table 4.1*. For compact section, the minimum available bending moment is considered between yielding available bending moment $M_{n,y}$ and lateral-torsional buckling available bending moment $M_{n,LTB}$. For compact web and non-compact flange, the minimum available bending moment is considered between lateral-torsional buckling available bending moment $M_{n,LTB}$ and flange local buckling available bending moment $M_{n,FLB}$.

Table 4.1 Available bending moment of section

No.	Type of Section	Available bending moment
1	Compact Section	$M_n = \min (M_{n,y}, M_{n,LTB})$
2	Compact web with non-compact flange	$M_n = \min (M_{n,LTB}, M_{n,FLB})$

A. Compact section

A.1. Yielding

$$M_{n,y} = M_p = F_y Z_x \quad (4.25)$$

Where $M_{n,y}$ = available bending moment for yielding

Z_x = plastic section modulus about the x axis.

A.2. Lateral Torsional Buckling

There are three cases to consider LTB depended on unbrace length L_b as Figure 4.3.

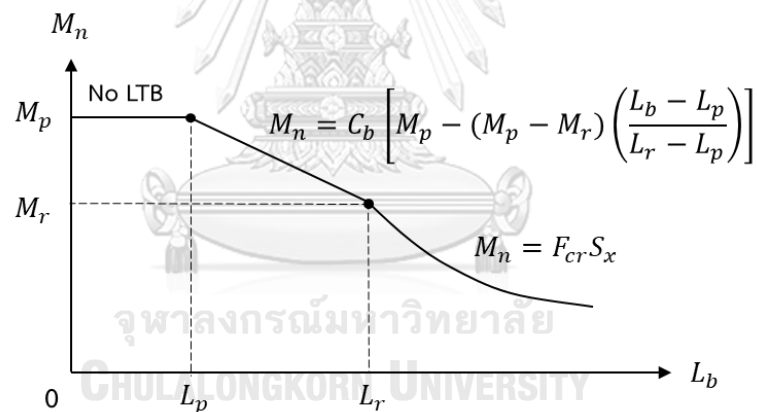


Figure 4.2 Graph of the available bending moment versus unbraced length

$$L_p = 1.76 r_y \sqrt{\frac{E}{F_y}} \quad (4.26)$$

Where L_p = limiting unbrace length for elastic analysis that LTB doesn't apply

r_y = radius of gyration about y-axis

$$L_r = 1.95 r_{ts} \frac{E}{0.7 F_y} \sqrt{\frac{Jc}{S_x h_0} + \sqrt{\left(\frac{Jc}{S_x h_0}\right)^2 + 6.76 \left(\frac{0.7 F_y}{E}\right)^2}} \quad (4.27)$$

Where L_r = limiting unbrace length for inelastic LTB

$$r_{ts}^2 = \frac{\sqrt{I_y C_w}}{S_x}$$

h_0 = distance between flange centroids = $h - t_f$ for W-section

$c = 1$ for W-section

(a) When $L_b \leq L_p$, the limit state of lateral-torsional buckling doesn't apply

(b) When $L_p < L_b \leq L_r$

$$M_{n,LTB} = C_b \left(M_p - (M_p - 0.7F_y S_x) \left(\frac{L_b - L_p}{L_r - L_p} \right) \right) \quad (4.28)$$

Where C_b = lateral-torsional buckling modification factor calculated as Eq. (4.29)

S_x = elastic section modulus taken about x-axis

$$C_b = \frac{12.5M_{max}}{2.5M_{max} + 3M_A + 4M_B + 3M_C} R_m \quad (4.29)$$

Where M_{max} = absolute maximum moment between unbraced length

M_A, M_B and M_C = absolute moment at $\frac{1}{4}, \frac{1}{2}$ and $\frac{3}{4}$ of the length

$R_m = 1$ for doubly symmetric section

(c) When $L_b > L_r$

$$M_{n,LTB} = F_{cr} S_x \quad (4.30)$$

$$F_{cr} = \frac{C_b \pi^2 E}{\left(\frac{L_b}{r_{ts}} \right)^2} \sqrt{1 + 0.078 \frac{Jc}{S_x h_0} \left(\frac{L_b}{r_{ts}} \right)^2} \quad (4.31)$$

B. Compact web with non-compact flange

B.1. Flange local buckling

$$M_{n,FLB} = F_y Z_x - (F_y Z_x - 0.7F_y S_x) \left(\frac{\lambda_f - \lambda_{pf}}{\lambda_{rf} - \lambda_{pf}} \right) \quad (4.32)$$

Where $M_{n,FLB}$ = available bending moment for flange local buckling

B.2. Lateral-torsional Buckling

LTB in B.2. can uses equation the same as section A.2.

4.4 Planer Steel Frame Optimization

4.4.1 Element Connection

For structural optimization problems, the connection between beam to beam and

column to the beam is designed to have a fixed connection that resists both axial and moment force. In contrast, X-bracing has pinned end, the element designed to resist only axial force.

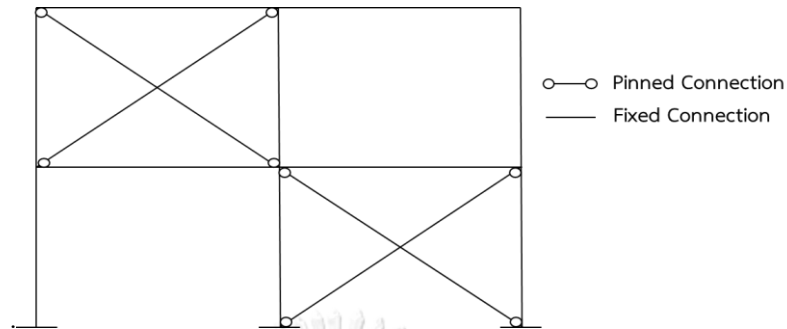


Figure 4.3 Layout of the frame connection

4.4.2 Available Section for Optimization

The available sections using for optimization are the section with their geometry base on (AISC, 2011). The section selected from W6 to W40. Total section equal 267 sections as *Table 4.2*. However, this optimization uses BPSO, a binary system that carries the available sections for the solution. So, the bit using to carry 267 is 9 bits with a total of 512 possible solutions. So, it is necessary to create the 245 fake sections to fill the full blank positions. The cross-sectional area of fake sections is assumed to be 0. It should be noted that the cross-sectional optimization area of some elements is not select from all 267 sections. The binary code is regenerated depending on the size of the available sections in the same way that describes above.

Table 4.2 Available AISC section data

Index	Section Name	Cross-sectional area (in^2)	Binary code
1	W6 x 8.5	2.52	00000000
2	W6 x 9	2.68	00000001
3	W8 x 10	2.96	00000010
⋮	⋮	⋮	⋮
265	W14 x 730	215	100001000
266	W36 x 798	236	100001001
267	W14 x808	238	100001010

4.4.3 Loads

The load observed in this research includes both vertical and lateral load. There is no factor multiplied by load magnitude considering in this research. The vertical load is the uniform distributed load applied on beams. In contrast, the lateral load is the point load applied to the left end of each structure floor.



CHAPTER 5

NUMERICAL EXAMPLES

5.1 General

There are two parts determined in this chapter. The first part is study for the best inertia weight improving BPSO. The second part is study on structural optimization problems. The best inertia weight is applied to BPSO for solving these problems.

5.2 Inertia Weight Studies

The samples of inertia weights are constant inertia weight 0.9, 0.92, 0.94, 0.96, 0.98, 1.00 and 1.02, and linear increasing inertia weight from 0.4 to 0.9. This research applies the samples on six benchmark functions (Tang, Li, Suganthan, Yang, & Weise, 2009) shown in *Table 5.1* with 30 runs and 3000 number of analysis for one run. Ten unknown variables are applied for all benchmark functions, except F5 function studies on two unknown variables. Each unknown variable requires 15 bits to carry all possible solutions. The number of particles used in BPSO is 50 particles.

Table 5.1 Benchmark functions with range and optimal value

Function Name	Equation	Range	f_{min}
F ₁ : Sphere	$\min f(x) = \sum_{i=1}^n x_i^2$	[-100,100]	0
F ₂ : Rosenbrock's	$\min f(x) = \sum_{i=1}^{n-1} [100(x_{i+1} - x_i^2)^2 + (x_i - 1)^2]$	[-200,200]	0
F ₃ : Rastrigin's	$\min f(x) = 10n + \sum_{i=1}^n [x_i^2 - 10\cos(2\pi x_i)]$	[-5.12,5.12]	0
F ₄ : Griewank's	$\min f(x) = \frac{1}{4000} \sum_{i=1}^n x_i^2 - \prod_{i=1}^n \cos\left(\frac{x_i}{\sqrt{i}}\right) + 1$	[-600,600]	0
F ₅ : Schaffer's F6	$\min f(x) = 0.5 - \frac{(\sin\sqrt{x_1^2 + x_2^2})^2 - 0.5}{[1 + 0.001(x_1^2 + x_2^2)]^2}$	[-100,100]	0
F ₆ : Ackley's	$\min f(x) = -20 \exp\left(-0.2 \sqrt{\frac{1}{n} \sum_{i=1}^n x_i^2}\right) - \exp\left(\frac{1}{n} \sum_{i=1}^n \cos(2\pi x_i)\right) + 20 + e$	[-32,32]	0

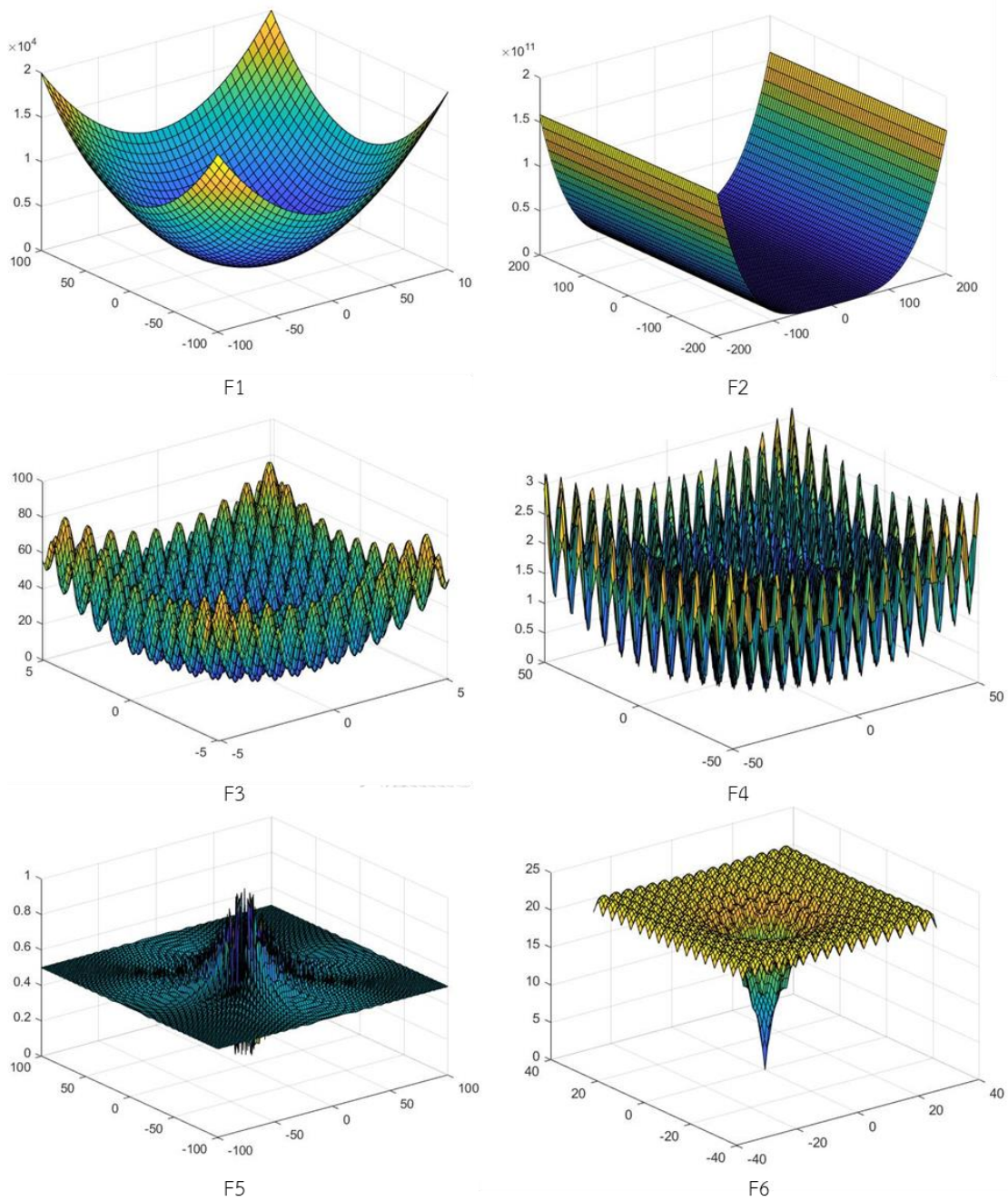


Figure 5.1 Benchmark functions with two unknown variables

The best sample of inertia weight is constant inertia weight 0.98. The reason for selecting this value is inertia weight 0.98 can reach to the lowest solution for all functions compared with others. The results of this sample for all functions are almost the optimal solution, except function F2. In addition, the standard deviations for all functions shown the dispersion of data for all runs are also the lowest value. In summary, solutions obtained from all runs are close to the others. It can be

concluded that inertia weight 0.98 is the best value in both accuracy and precision terms. So, this value is applied in the BPSO algorithm to optimize the structural optimization problems. The linear decreasing inertia weight from 0.9 to 0.4, the inertia weight value was suggested by PSO authors, gives the worst value for applying in BPSO. The results of this inertia weight for all benchmark functions are so far from the optimum values.

Table 5.2 Minimum fitness of inertia weight on benchmark functions

Inertia Weight	F ₁	F ₂	F ₃	F ₄	F ₅	F ₆
0.90	3.75	7801.85	7.34	0.80	0.00246	1.70
0.92	1.63	477.33	6.17	0.64	0.00246	0.63
0.94	0.12	90.24	1.28	0.27	0.00246	0.25
0.96	0.00434	9.53	0.01	0.11	0.00246	0.03
0.98	9.32E-05	6.96	4.84E-05	0.01	0.00246	3.96E-03
1.00	9.32E-05	7.34	1.24	0.03	0.00246	3.96E-03
1.02	9.32E-05	8.26	2.00	0.01	0.00246	3.96E-03
0.9 to 0.4	113.39	1958397.03	24.41	1.73	0.00246	4.92

Table 5.3 Standard deviation of inertia weight on benchmark functions

Inertia Weight	F1	F2	F3	F4	F5	F6
0.9	4.59	37877.70	2.77	0.08	0.00	0.44
0.92	1.02	8692.70	2.26	0.10	0.00	0.44
0.94	0.21	3975.95	1.96	0.11	0.00	0.11
0.96	0.01	786.38	1.66	0.09	0.00	0.02
0.98	0.00	460.86	1.32	0.05	0.00	0.00
1	0.00	4190.81	3.74	0.06	0.00	0.71
1.02	0.00	3823.98	3.12	0.11	0.00	0.90
0.9 to 0.4	110.80	6036157.12	4.69	0.69	0.00	1.05

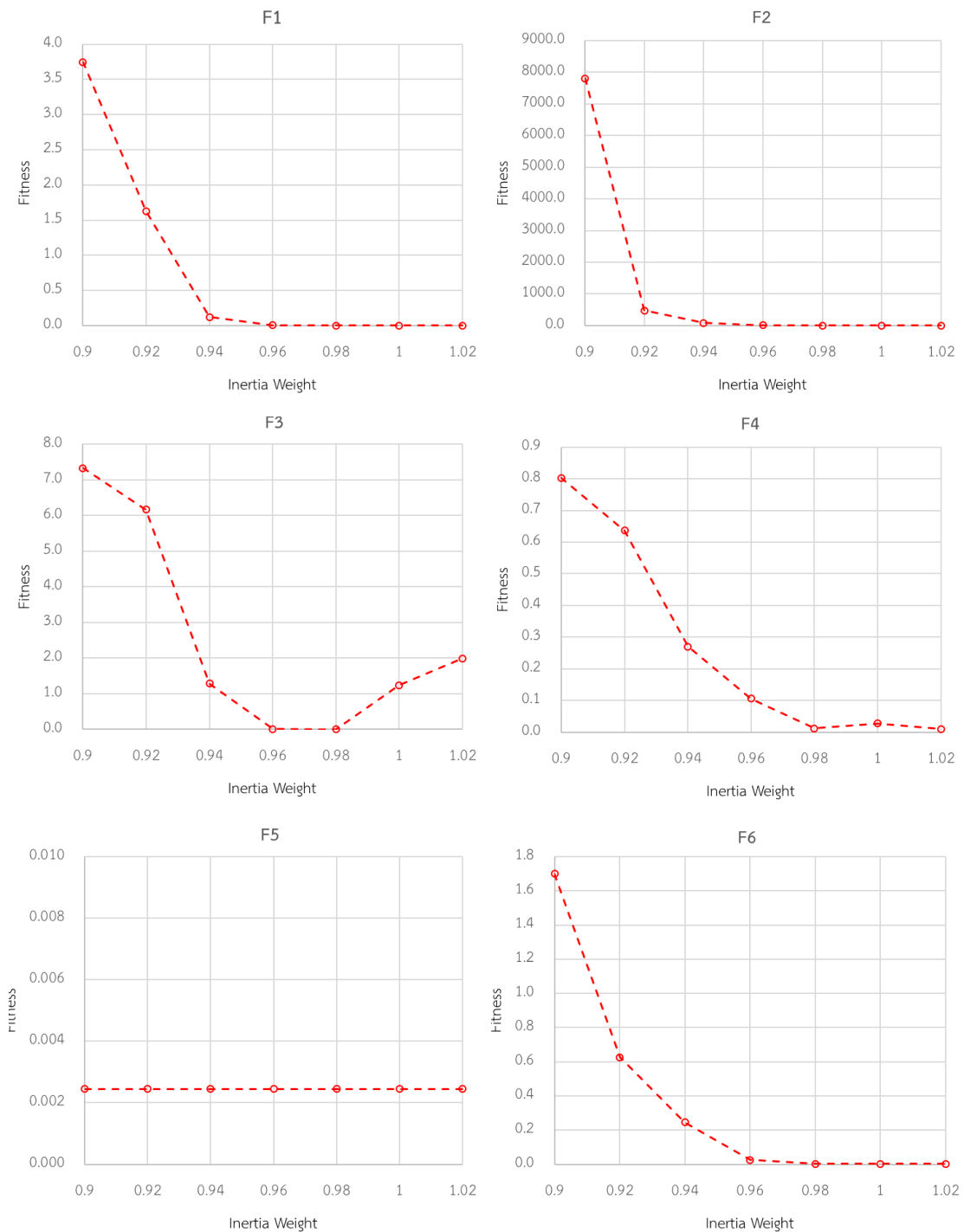


Figure 5.2 Curve of minimum fitness versus constant inertia weight

5.3 Structural Optimization

In this section, BPSO is applied in three structural optimization problems. There are two types of structure studied in this section: the unbraced frame and the X-bracing braced frame. The properties of braced frame are the same as unbraced

frame. The addition is braced element including in the structure. Only sizing optimization is applied for column and beam elements while sizing, and topology optimization is applied for braced elements. The optimization is performed repeatedly 100 runs with 20,000 numbers of analysis. The number of particles used for BPSO is 50 particles.

5.3.1 Two-Bays, Three-Stories Frame

The example of a two-bays, three-stories frame consists of 15 elements designed by (Wood, Beaulieu, & Adams, 1976). Displacement constraint is not considered in this example. The modulus of elasticity E is 29,000 ksi, and yield stress F_y is 36 ksi. Beam elements are optimized with all 267 available W-shape sections, while column elements are restricted to W10 sections with 18 sections. No. of bits using for beam element are 9 bits per element, and No. of bits using for column element are 5 bits per element. The elements are divided into two groups for optimization that is beam group, column group. The possible solutions to this problem are 2^{14} solutions. This example is applied only for moment-resisting frames with an effective length factor K_x is calculated for sway-permitted frame and K_y is assumed to be braced out of a plane is 1.0. Each column is considered unbraced along its length, while each beam has unbraced length of 1/6 of its span length. BPSO optimized the minimum weight and compared to other algorithms from previous research GA (Pezeshk et al., 2000), ACO (Camp et al., 2005), and SBO (Farshchin et al., 2018).

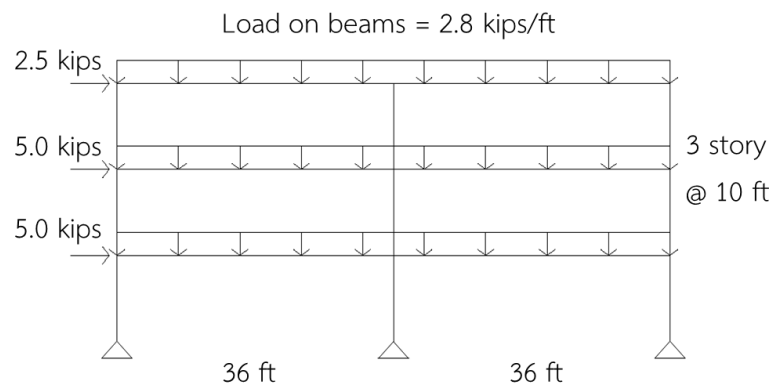


Figure 5.3 Layout and load of two-bays, three-stories frame

Table 5.4 Two-bays, three-stories frame design

Element Group	Optimum	GA	ACO	SBO	Present Work
Beam	W24 x 62	W24 x 62	W24 x 62	W24 x 62	W24 x 62
Column	W10 x 60	W10 x 60	W10 x 60	W10 x 60	W10 x 60
Weight (lb)	18,792	18,792	18,792	18,792	18,792
Mean (lb)	-	22,080	19,163	18,792	18,792
Standard Deviation (lb)	-	5818	1693	0	0
Number of Analysis	-	900	880	502	3
Number of Runs	-	30	100	100	100
% Optimal Found	-	20%	84%	100%	100%

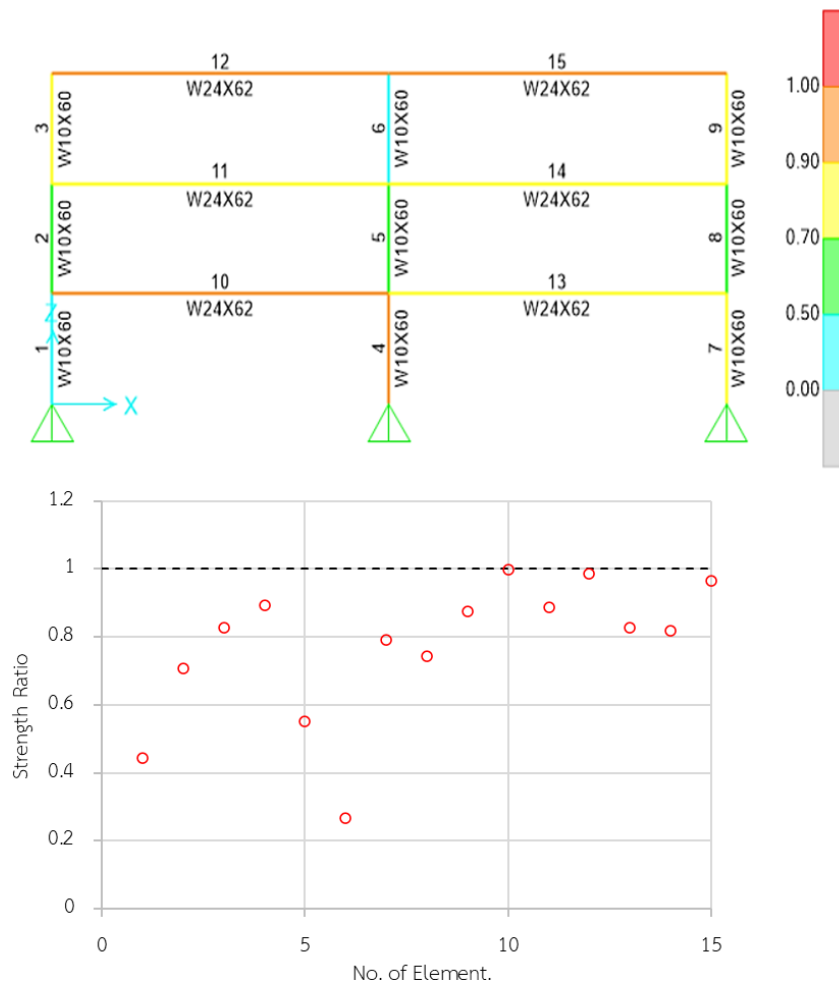


Figure 5.4 Strength ratio of elements for two-bays, three-stories frame

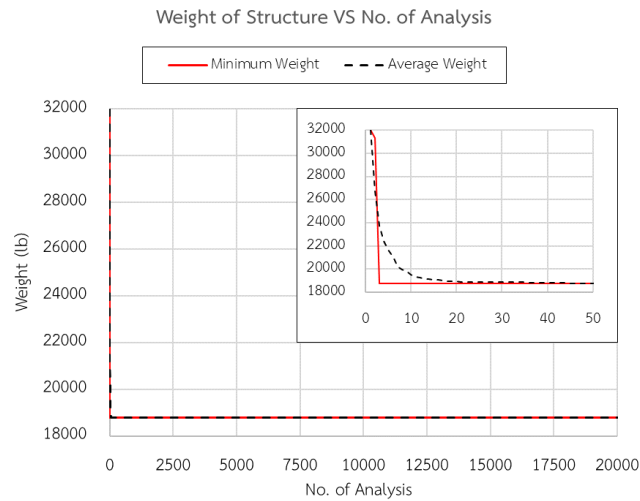


Figure 5.5 Convergence curve for two-bays, three-stories frame

The first structure is a two-bay, three-stories frame. The problem is optimized with only strength constraints. The result from the BPSO algorithm is compared to GA, ACO, and SBO algorithms. The result shows that all practical algorithms can reach the optimal value 18,792 lb. When we consider the percent of optimal value found, SBO and BPSO are the best two algorithms that can reach 100% optimal value found under 100 runtimes repeating. In addition, we consider more in No. of analysis the algorithms found the minimum weight. BPSO was found to have the fastest convergence that is only three iterations done. So, BPSO worked the best for optimization in the first example. From *Figure 5.4*, the maximum strength ratio for minimum weight structure occurs at element No.10 with a strength ratio of 0.9997.

5.3.2 One-bay, Ten-Stories Frame

The example of a one-bay, ten-stories unbraced frame as *Figure 5.6 (a)* consists of 30 elements. The modulus of elasticity E is 29,000 ksi, and the yield stress F_y is 36 ksi. Beam elements are optimized with all 267 available W-shape sections with an unbraced length of $l/5$, while column elements are restricted to W12 to W14 sections with a total of 66 sections and unbraced length along its length. K_y is assumed to be braced out of the plane is 1.0. There are two drift constraint conditions to consider in this frame: drift at the root and drift at all stories. BPSO optimized the minimum weight and compared to other algorithms from previous research GA (Pezeshk et al., 2000), ACO (Camp et al., 2005), TLBO (Toğan, 2012), and SBO (Farshchin et al., 2018).

The geometry, material properties, grouping, and available sections for a braced frame are the same as unbraced frame. The additional is considering the bracing system in terms of topology and sizing cross-sectional area. X-shape bracing with ten elements follows by no. of stories are divided into one element per group as *Figure 5.6 (b)*. The braced element section is restricted from W6 to the W10 section (33 sections) with an unbraced length of 1/2. The braced frame is optimized under one drift constraint condition that is drift at all stories. There are two groupings of beam and column conditions considered for braced frame: grouping the same as the original unbraced frame and grouping with the finer group as *Figure 5.6 (c)*.

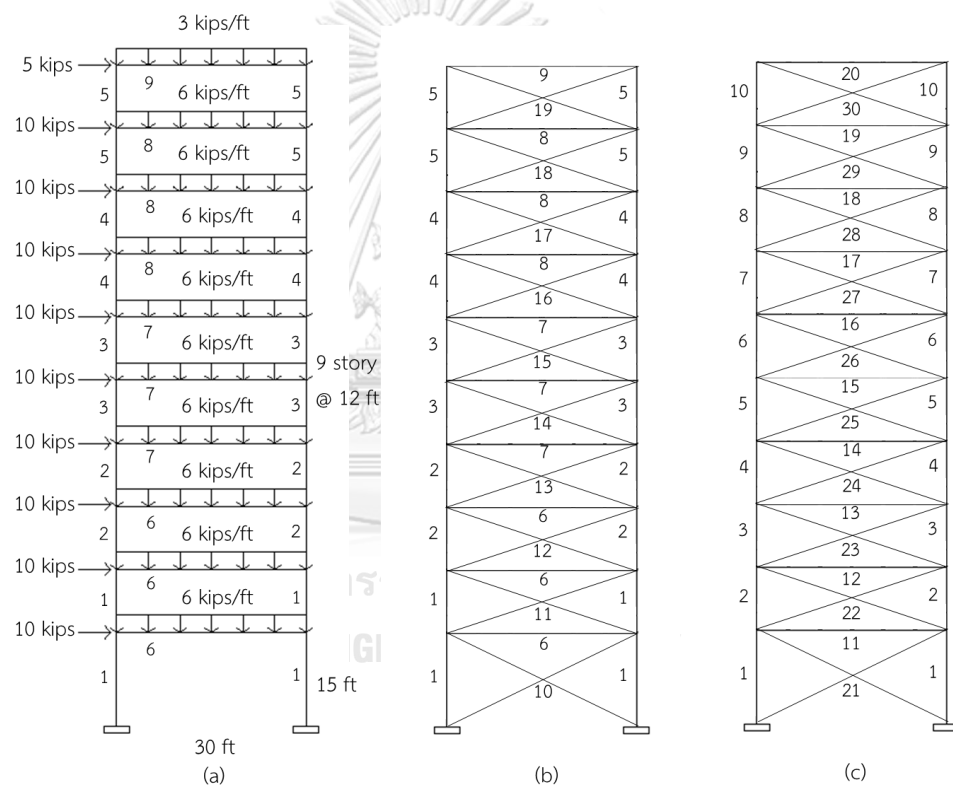


Figure 5.6 Layout and load of one-bay, ten-stories frame (a) Unbraced frame, (b) Braced frame with original grouping (c) Braced frame with new grouping

Table 5.5 Types and condition of structure for one-bay, ten-stories frame

No.	Types of Structure	Grouping	Drift constraint
1	Unbraced frame	Original	At roof
2	Unbraced frame	Original	All stories
3	Braced frame	Original	All stories
4	Braced frame	New	All stories

Table 5.6 One-bay, ten-stories frame design (No.1)

Element Group	Frame 1: Considering story drift at roof			
	ACO	TLBO	SBO	Present Work
1	W14 x 233	W14 x 233	W14 x 233	W14 x 233
2	W14 x 176	W14 x 176	W14 x 176	W14 x 176
3	W14 x 145	W14 x 145	W14 x 145	W14 x 145
4	W14 x 99	W14 x 99	W14 x 99	W14 x 99
5	W12 x 65	W12 x 65	W14 x 61	W14 x 61
6	W30 x 108	W30 x 108	W30 x 108	W30 x 108
7	W30 x 90	W30 x 90	W30 x 90	W30 x 90
8	W27 x 84	W27 x 84	W27 x 84	W27 x 84
9	W21 x 44	W21 x 44	W18 x 46	W18 x 46
Weight (lb)	62,562	62,562	62,430	62,430
Mean (lb)	63,308	-	63,244	63,907.14
SD (lb)	684	-	706.84	1,190.45
No. of Analysis	8,300	4,000	11,677	5,408
No. of Runs	100	-	100	100

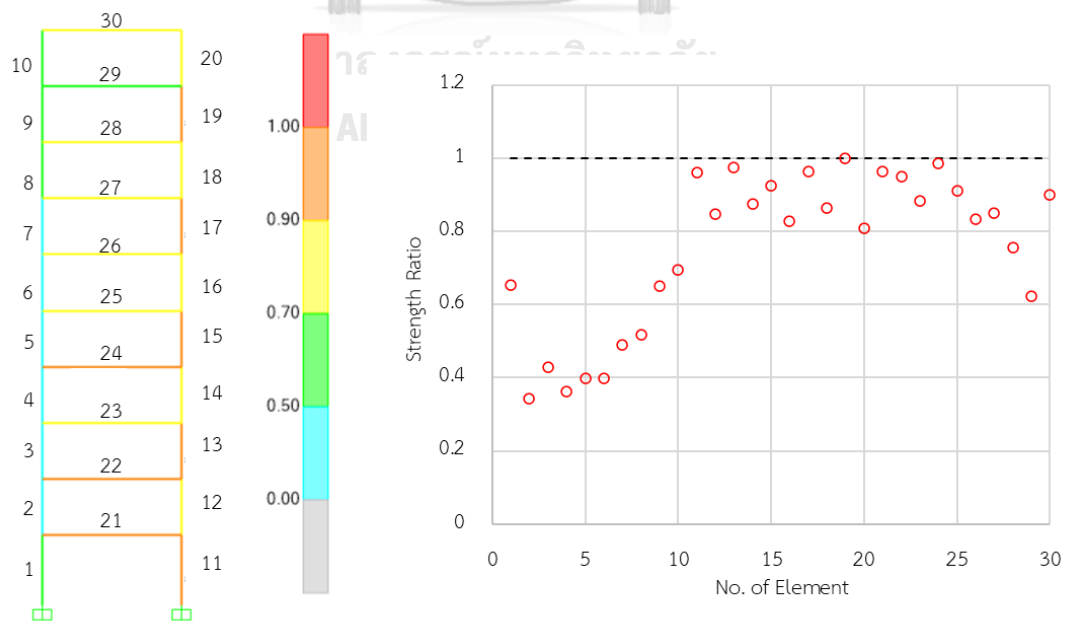


Figure 5.7 Strength Ratio of elements for one-bay, ten-stories frame (No.1)

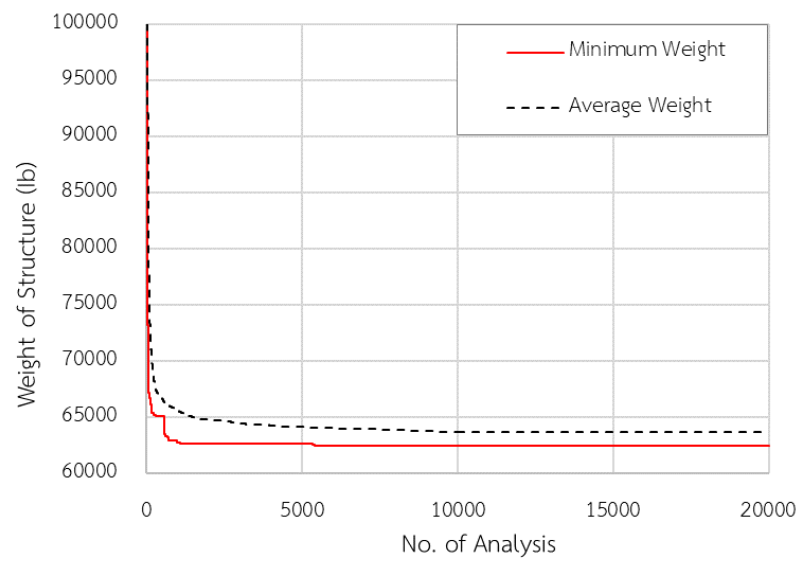


Figure 5.8 Convergence curve for one-bay, ten-stories frame (No.1)

Table 5.7 One-bay, ten-stories frame design (No.2)

Element Group	Frame No.2: Considering story drift at all stories		
	GA	SBO	Present Work
1	W14 x 233	W14 x 233	W14 x 233
2	W14 x 176	W14 x 176	W14 x 176
3	W14 x 159	W14 x 159	W14 x 159
4	W14 x 99	W14 x 99	W14 x 99
5	W12 x 79	W14 x 61	W14 x 61
6	W33 x 118	W33 x 118	W33 x 118
7	W30 x 90	W30 x 90	W30 x 90
8	W27 x 84	W27 x 84	W27 x 84
9	W24 x 55	W18 x 46	W18 x 46
Weight (lb)	65,136	64,002	64,002
Mean (lb)	-	65,880	65,806.60
SD (lb)	-	832.95	1,123.57
No. of Analysis	3,000	12,691	4,647
No. of Runs	-	100	100

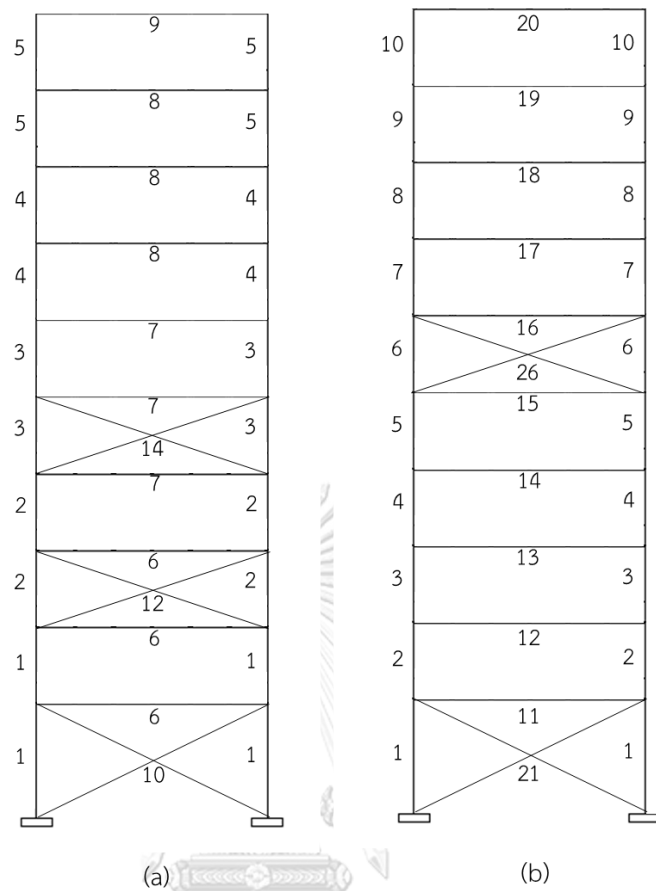


Figure 5.9 Layout of braced element for minimum weight of one-bay, ten-stories frame (a) Frame No.3 (b) Frame No.4

Table 5.8 One-bay, ten-stories frame design (No.3)

Element Group	Present Work	Element Group	Present Work	Element Group	Present Work
1	W14X211	5	W14x61	9	W18x46
2	W14x159	6	W27x84	10	W8X24
3	W14x132	7	W24X84	12	W8X24
4	W14X99	8	W30x90	14	W10x22
Weight (lb)			62,224.58		
Mean (lb)			65,228.65		
SD (lb)			1,668.340		
No. of Analysis			4,852		
No. of Runs			100		

Table 5.9 One-bay, ten-stories frame design (No.4)

Element Group	Present Work	Element Group	Present Work	Element Group	Present Work
1	W14x145	9	W14x68	17	W27x84
2	W14x211	10	W14x53	18	W24x76
3	W12x210	11	W30x90	19	W24x76
4	W14x159	12	W30x116	20	W21x44
5	W12x152	13	W33x118	21	W8x24
6	W14x99	14	W30x99	26	W8x18
7	W12x120	15	W27x84		
8	W12x96	16	W24x68		
Weight (lb)				60,805.16	
Mean (lb)				65,028.05	
SD (lb)				1,819.48	
No. of Analysis				1,7078	
No. of Runs				100	

The second structure of testing is a one-bay, ten-stories structure. For this structure, there are two cases of conditions for drift constraint. The first case (Frame No. 1) is constrained drift at only the roof stories. BPSO algorithm is compared with ACO, TLBO, and SBO algorithm. With the same 100 runtimes except for TLBO with no runtime information, SBO and BPSO gave the lowest weight with 62,430 lb. The standard deviation is considered only for ACO, SBO, and BPSO that have the same runtimes. It shows that ACO has the lowest SD while BPSO gets the largest standard deviation. So, the precision term BPSO is the worst. However, BPSO is the best one in convergence. From the minimum weight structure of BPSO, the maximum strength ratio is 0.9999 occurring in the 9th stories beam. Story drift ratio at the roof is 0.3125.

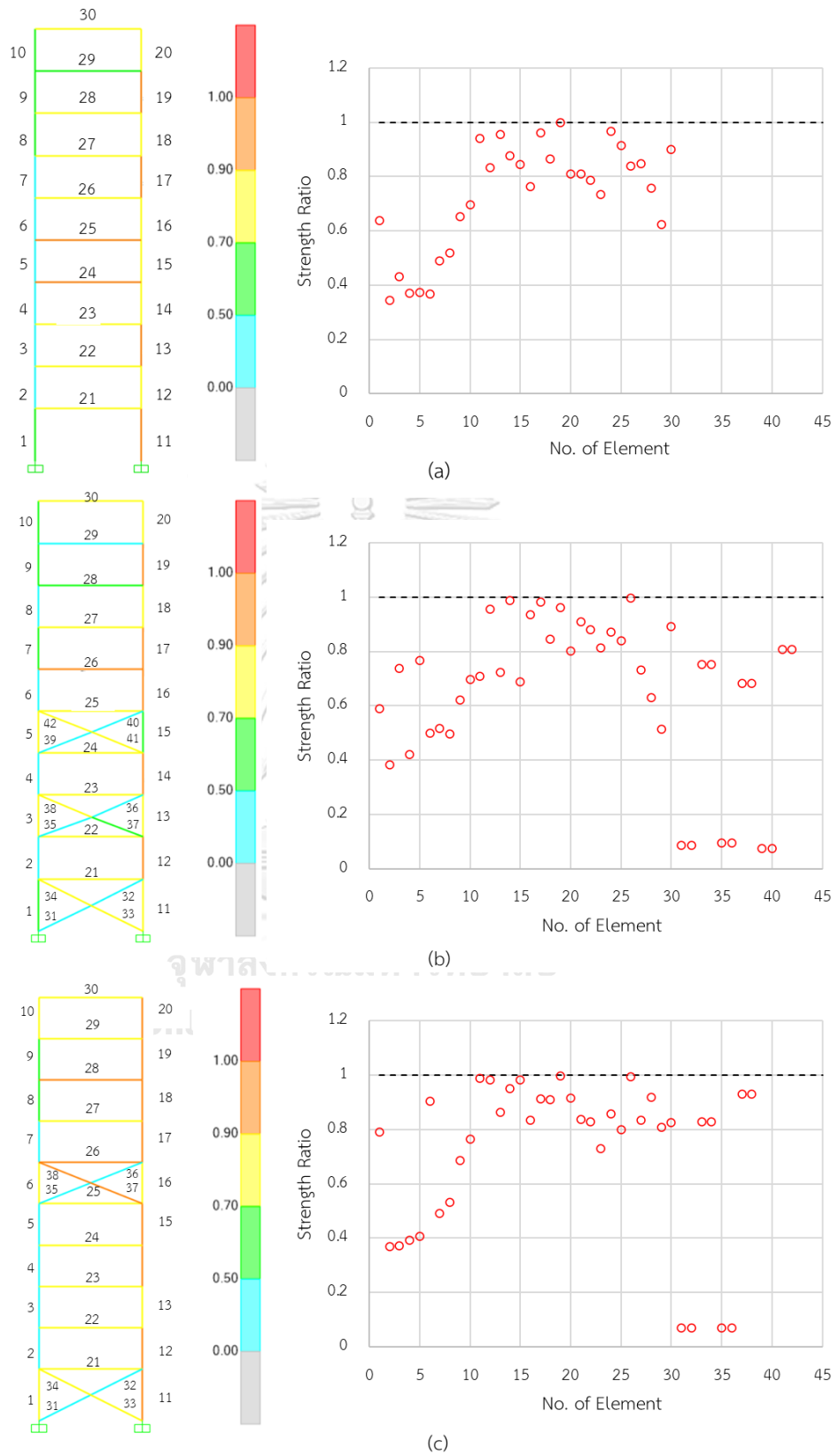
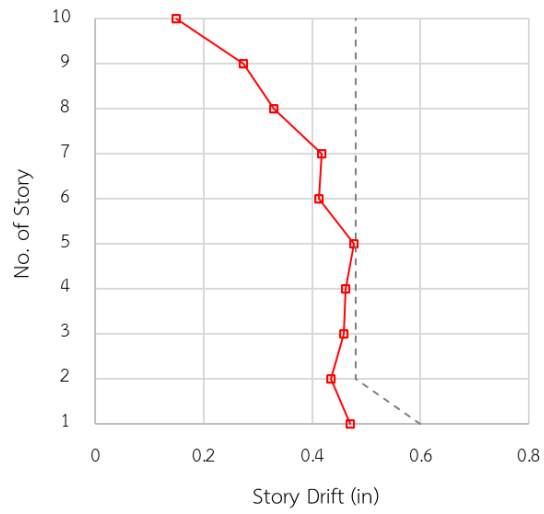
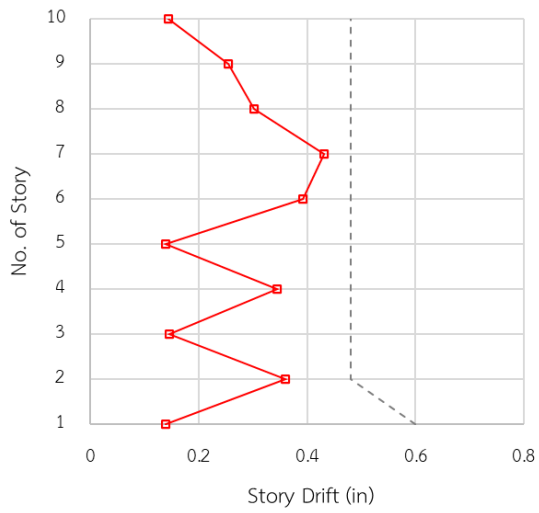


Figure 5.10 Layout and strength ratio of elements for one-bay, ten-stories frame (a) frame No.2, (b) frame No.3 and (c) frame No.4

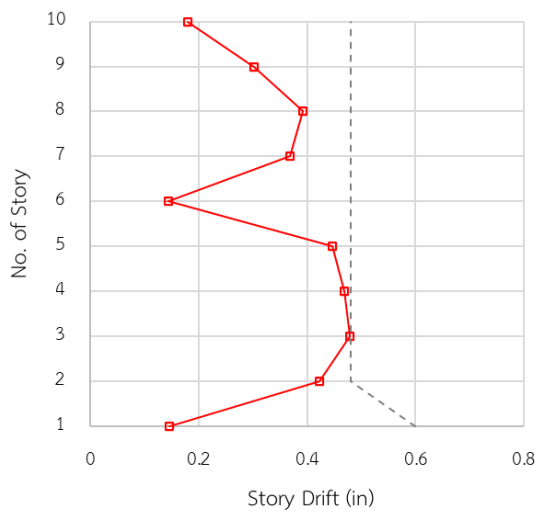


(a)



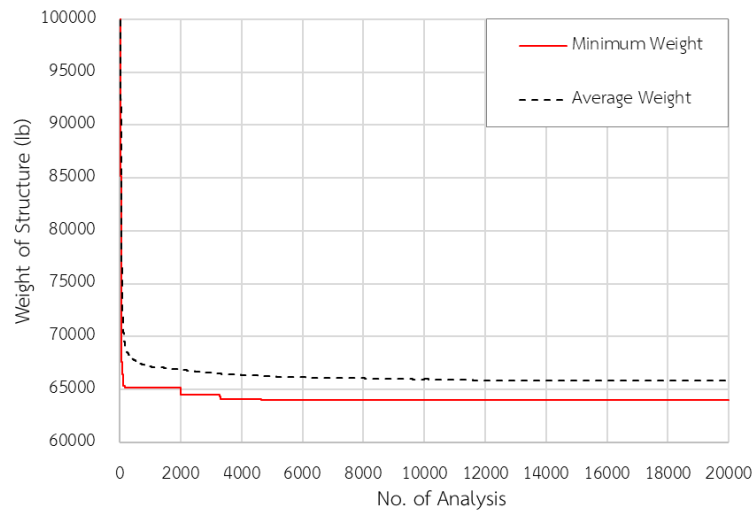
(b)

C

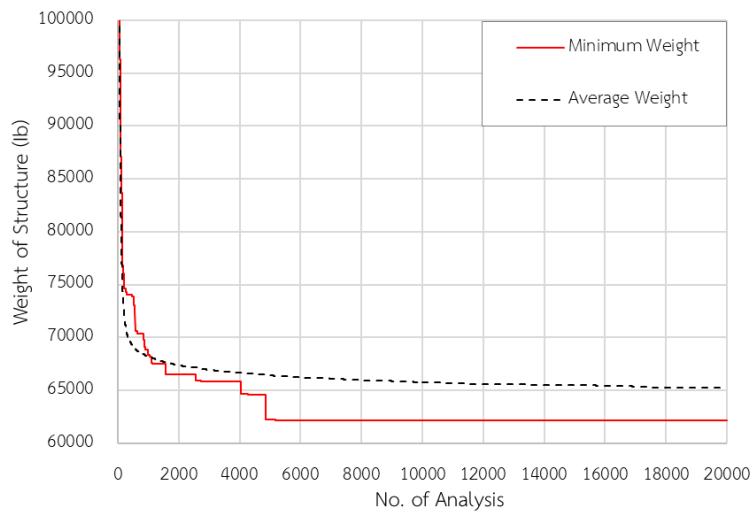


(c)

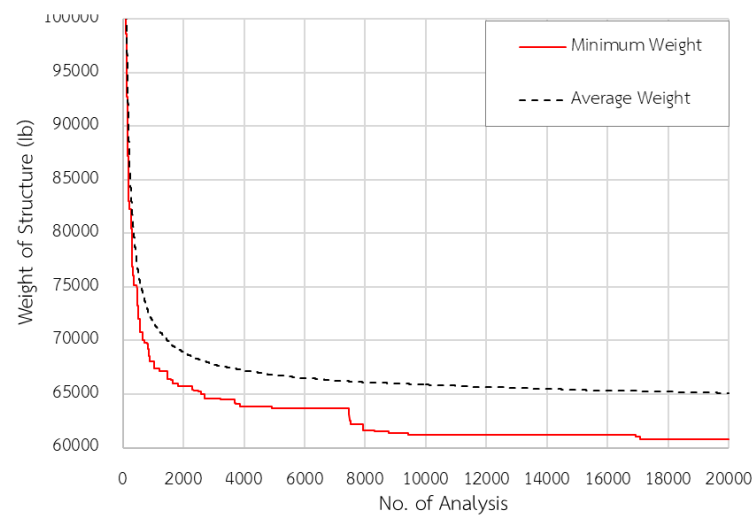
Figure 5.11 Story drift for one-bay, ten-stories frame (a) frame No.2, (b) frame No.3 and (c) frame No.4



(a)



(b)



(c)

Figure 5.12 Convergence Curve for one-bay, ten-stories frame (a) frame No.2, (b) frame No.3 and (c) frame No.4

The second case (frame No.2) considers drift for all stories. BPSO is compared with GA and SBO. BPSO and SBO get the lowest weight, 64,002 lb, by using 100 runtimes. GA with no information of runtimes gives the worse weight than the others. The standard deviation is considered only for SBO and BPSO that have the same runtimes. It shows that SBO has the lowest SD while BPSO gets the largest Standard deviation. For the precision term, BPSO is the worst. However, BPSO is the best one in convergence. From the minimum weight structure of BPSO, the maximum strength ratio is 0.9998, which happened in the 9th stories beam. The maximum drift ratio is 0.9999, which happened in the 5th story. The minimum weight of the brace frame using the original grouping (frame No.3) is 62,224.58 lb. This weight is lower than the unbraced frame with the same grouping, 2.78%. The maximum strength ratio is 0.9970, which happened 6th story beam. The maximum drift ratio is 0.9997, which happened in the 7th story. For the braced frame with finer grouping (frame No.4), the minimum weight is 60,805.16 lb that is less than the minimum weight of the braced frame with the original grouping of 2.28%. The maximum strength ratio is 0.9960, which happened in the right column of story 9th. The maximum drift ratio is 0.9999, which happened in 3rd story

5.3.3 Three-Bays, Twenty-Four-Stories Frame

The example of three-bays, twenty-four-stories unbraced frame as in *Figure 5.13* by (Davison & Adams, 1974). The modulus of elasticity E is 29,732 ksi, and the yield stress F_y is 33.4 ksi. Beam elements are optimized with all 267 available W-shape sections, while column elements are restricted to W14 sections with 37 sections. Unbraced length of beams and columns is along their length. K_y is assumed to be braced out of the plane is 1.0. Drift constraints are considered for all stories. BPSO optimized the minimum weight and compared to other algorithms from previous research HS (Degertekin, 2008), TLBO (Toğan, 2012), and SBO (Farshchin et al., 2018) For braced frames, the geometry, material properties, and grouping are the same as unbraced frames. Braced frame optimizations are the same as section 5.3.2.

Table 5.10 Types and condition for three-bays, twenty-four-stories frame

No.	Types of Structure	Grouping	Drift constraint
1	Unbraced frame	Original	All stories
2	Braced frame	Original	All stories
3	Braced frame	New	All stories

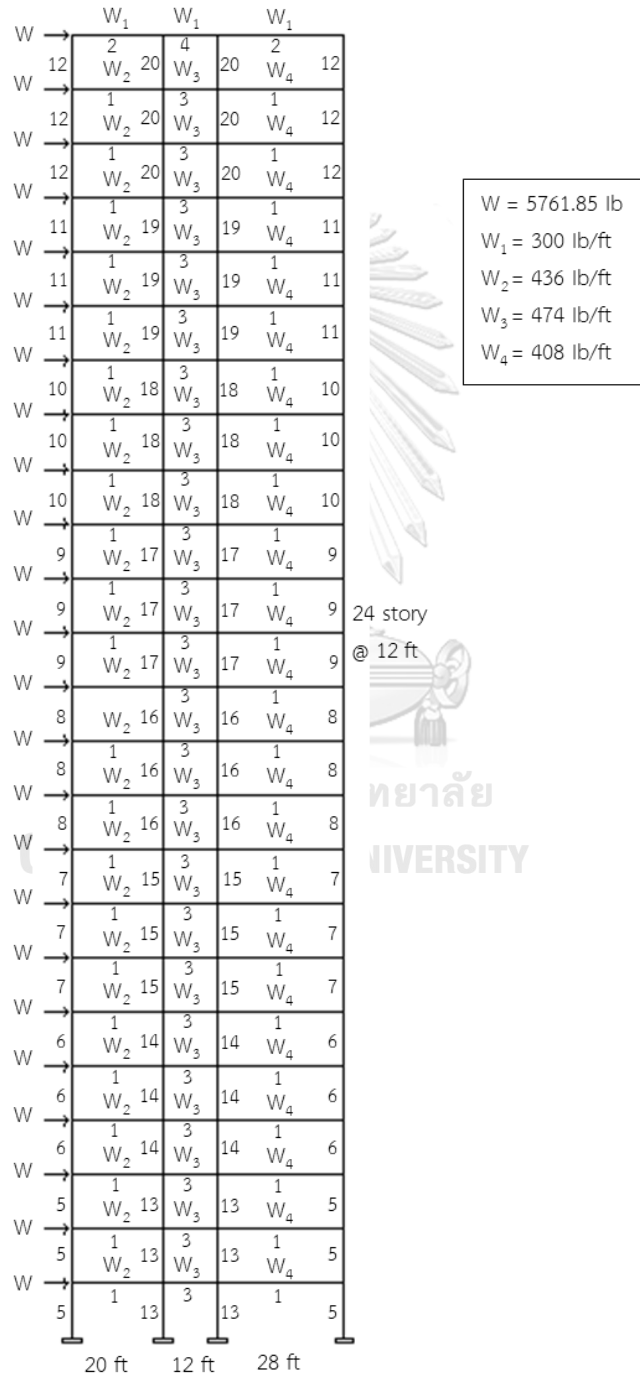


Figure 5.13 Layout and Load of three-bays, twenty-four-stories unbraced frame

Table 5.11 Three-bays, twenty-four-stories design (No.1)

Element Group	HS	TLBO	SBO	Present Work
1	W30 x 90	W30 x 90	W30 x 90	W30X90
2	W10 x22	W8 x 18	W8 x 18	W8x18
3	W18 x 40	W24 x 62	W21 x 48	W21X48
4	W12 x 16	W6 x 9	W6 x 8.5	W10x12
5	W14 x 176	W14 x 132	W14 x 152	W14x159
6	W14 x176	W14 x120	W14 x 120	W14x120
7	W14 x132	W14 x99	W14 x 109	W14x109
8	W14 x 109	W14 x82	W14 x 74	W14x61
9	W14 x 82	W14 x74	W14 x 82	W14x48
10	W14 x74	W14 x 53	W14 x 43	W14x48
11	W14 x 34	W14 x 34	W14 x 34	W14x43
12	W14 x 22	W14 x 22	W12 x 19	W14x26
13	W14 x 145	W14 x109	W14 x109	W14x99
14	W14 x 132	W14 x 99	W14 x 109	W14x109
15	W14 x 109	W14 x 99	W14 x 99	W14x99
16	W14 x 82	W14 x90	W14 x 99	W14x120
17	W14 x 61	W14 x 68	W14 x 68	W14x99
18	W14 x 48	W 14 x53	W14 x61	W14x61
19	W14 x 30	W14 x 34	W14 x 34	W14x43
20	W14 x 22	W14 x22	W14 x22	W14x26
Weight (lb)	214,896	203,124	202,422	205,056
Mean (lb)	222,620	-	209,560	224,152
SD (lb)	-	-	7,052	15,475
No. of Analysis	14,651	12,000	14,572	6,890
No. of Runs	100	-	100	100

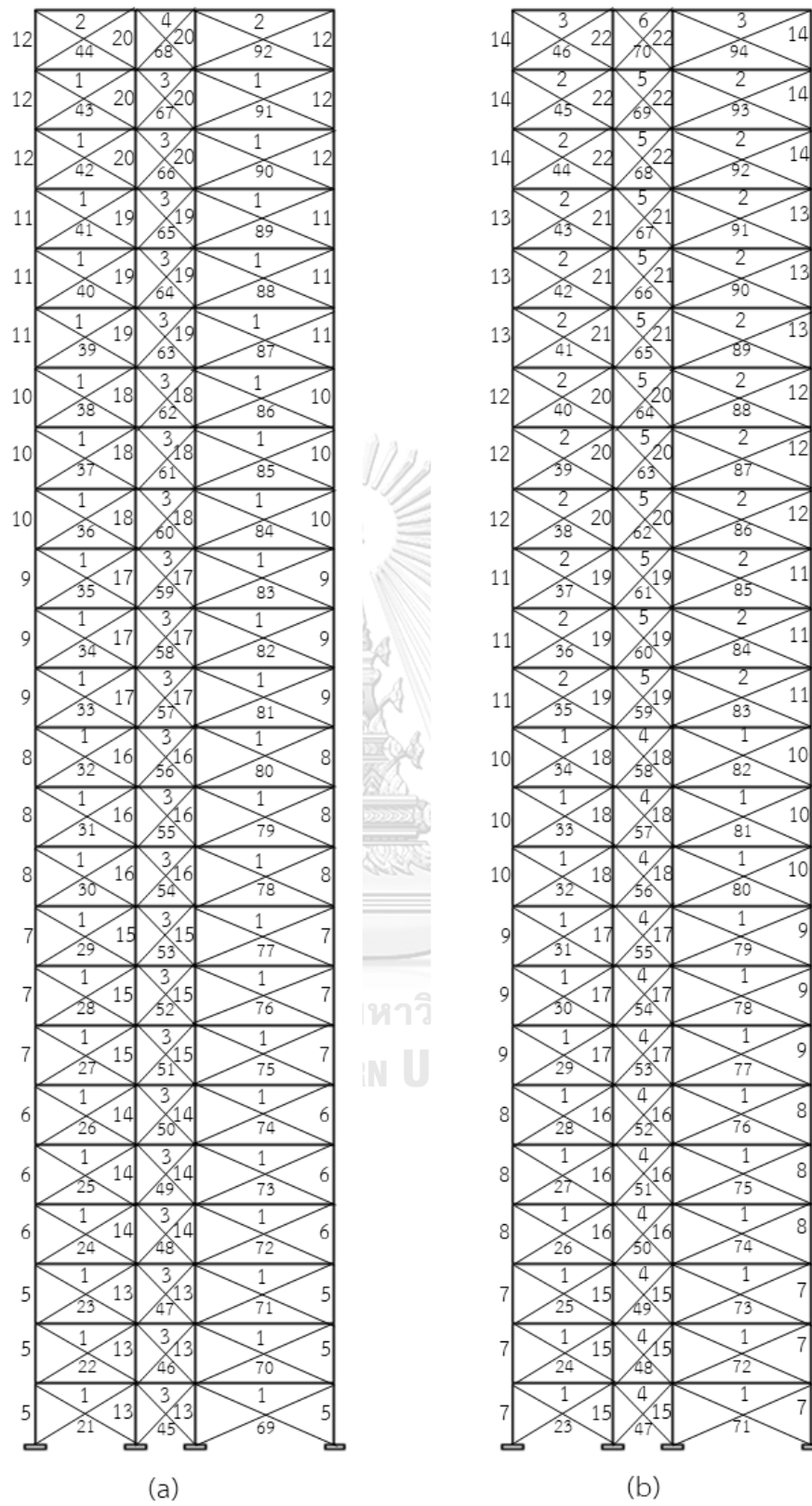


Figure 5.14 Layout and Load of three-bays, twenty-four-stories braced frame (a) initial grouping (b) new grouping

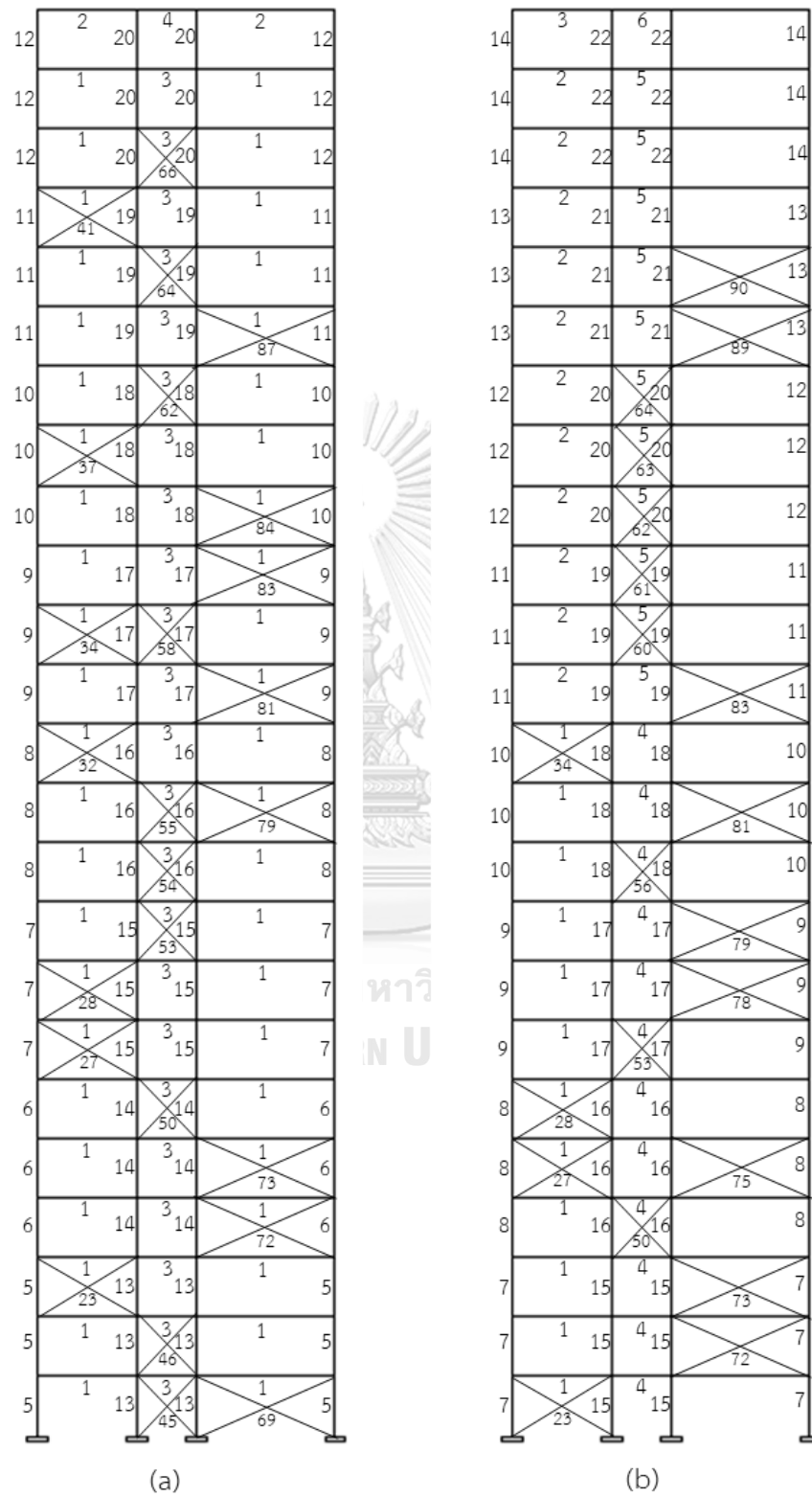


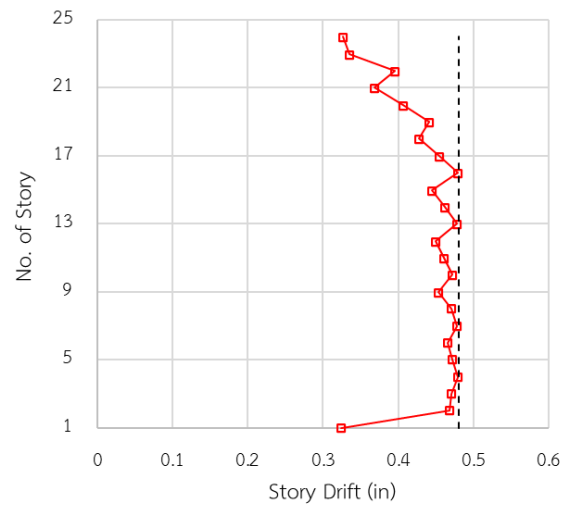
Figure 5.15 Layout of braced element for three-bays, twenty-four -stories (a) frame No.2 (b) frame No.3

Table 5.12 Three-bays, twenty-four-stories frame design (No.2)

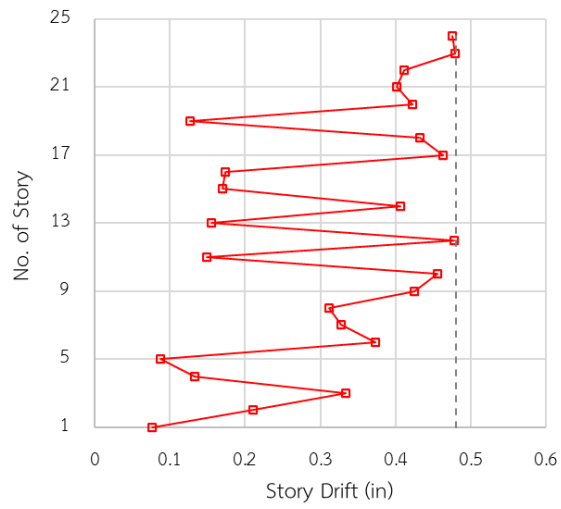
Element Group	Present Work	Element Group	Present Work	Element Group	Present Work	Element Group	Present Work
1	W16X36	13	W14x53	34	W8x15	66	W10x15
2	W8x18	14	W14x43	37	W8x15	69	W8x18
3	W10x22	15	W14x43	41	W8x18	72	W8x21
4	W8x10	16	W14x48	45	W10x39	73	W10x30
5	W14x99	17	W14x30	46	W10x30	79	W8x24
6	W14x99	18	W14x30	50	W8x18	81	W10x26
7	W14x61	19	W14x43	53	W10x19	83	W10x22
8	W14x68	20	W14x43	54	W8x28	84	W8x18
9	W14x68	23	W10x22	55	W6x9	87	W8x31
10	W14x43	27	W10x22	58	W8x28		
11	W14x48	28	W8x35	62	W8x13		
12	W14x22	32	W10x22	64	W8x10		
Weight (lb)						132,972	
Mean (lb)						176,326	
SD (lb)						18,187	
No. of Analysis						18,139	
No. of Runs						100	

Table 5.13 Three-bays, twenty-four-stories frame design (No.3)

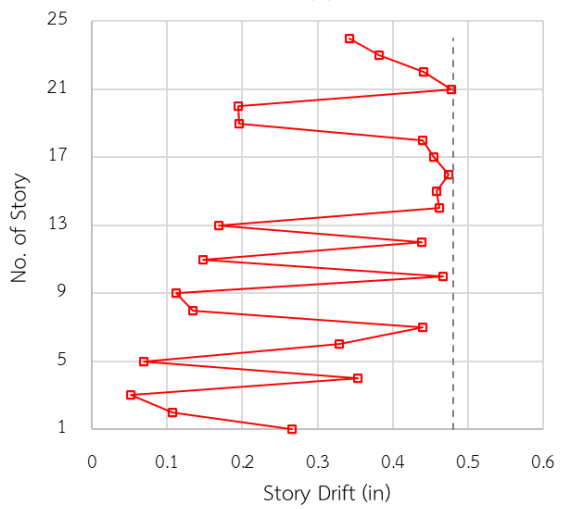
Element Group	Present Work	Element Group	Present Work	Element Group	Present Work	Element Group	Present Work
1	W12x26	12	W14x43	23	W8x18	64	W10x12
2	W24x62	13	W14x30	27	W10x22	72	W8x31
3	W14x22	14	W14x22	28	W8x21	73	W10x49
4	W12x26	15	W14x43	34	W8x18	75	W10x26
5	W12x16	16	W14x43	50	W8x18	78	W10x26
6	W16x31	17	W14x43	53	W8x13	79	W8x35
7	W14x120	18	W14x43	56	W10x26	81	W8x21
8	W14x82	19	W14x43	60	W8x15	83	W8x18
9	W14x99	20	W14x43	61	W8x15	89	W10x17
10	W14x61	21	W14x30	62	W6x9	90	W10x19
11	W14x48	22	W14x48	63	W10x12		
Weight (lb)					138,050		
Mean (lb)					178,475		
SD (lb)					17,873		
No. of Analysis					19,595		
No. of Runs					100		



(a)

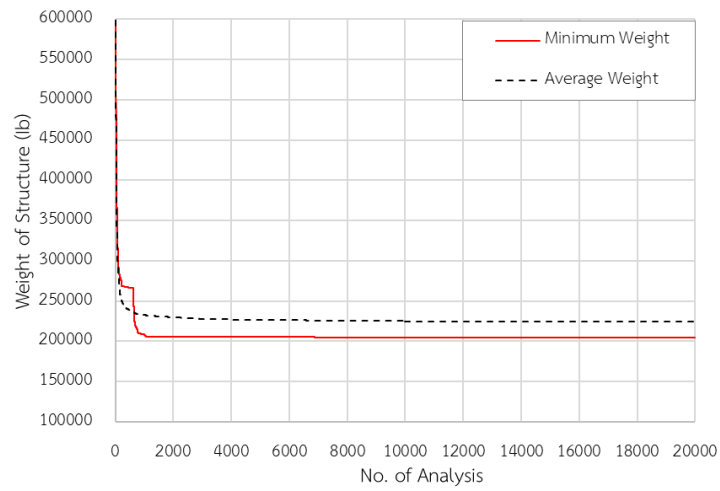


(b)

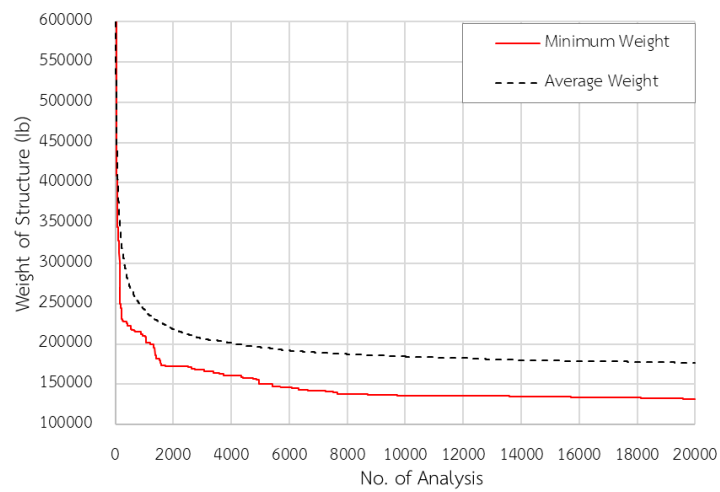


(c)

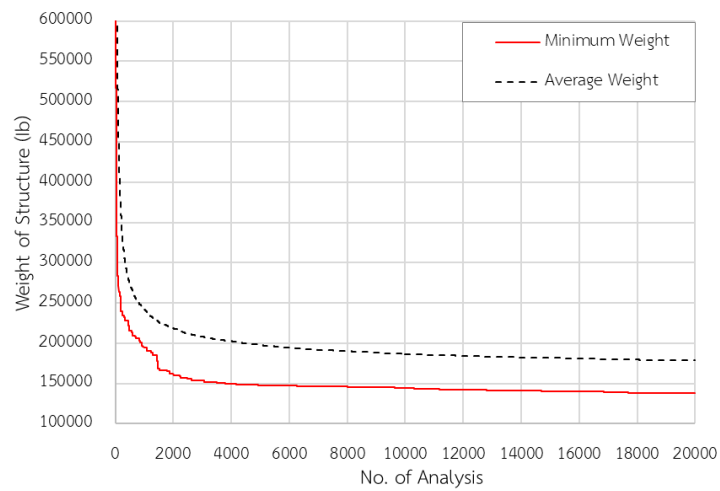
Figure 5.16 Story drift for three-bays, twenty-four-stories frame (a) frame No.1, (b) frame No.2 (c) frame No.3



(a)



(b)



(c)

Figure 5.17 Convergence curve for three-bays, twenty-four-stories frame (a) frame No.1 (b) frame No.2 (c) frame No.3

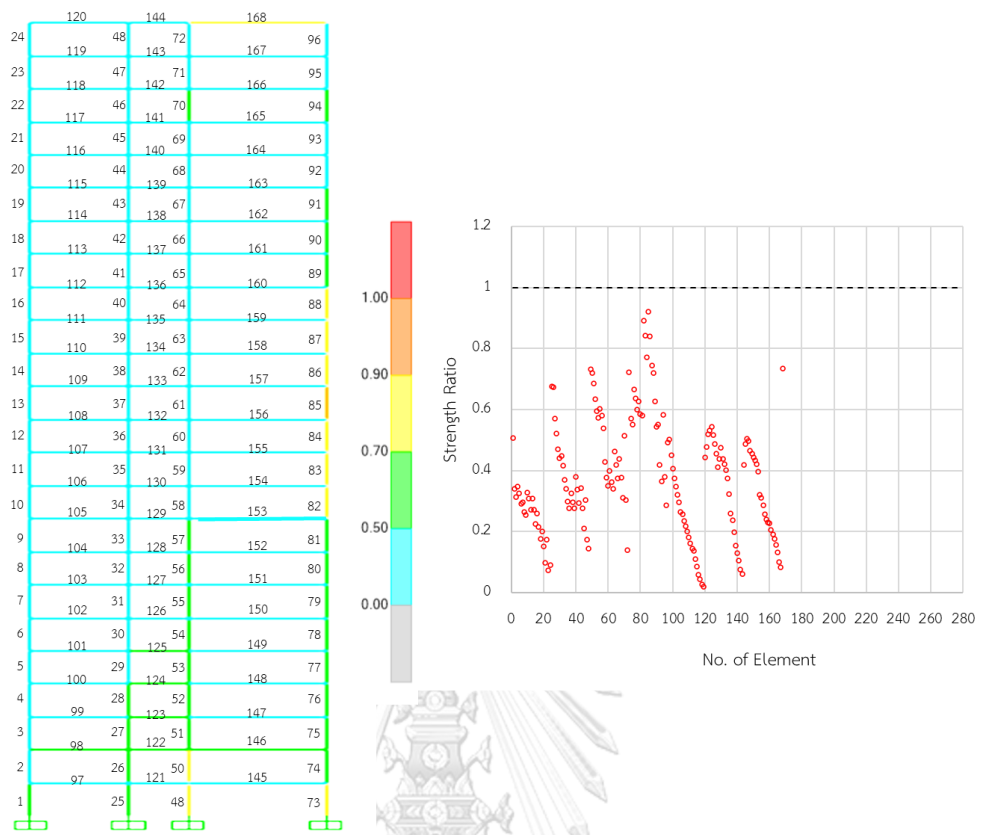


Figure 5.18 Element strength ratio for three-bays, twenty-four-stories frame (No.1)

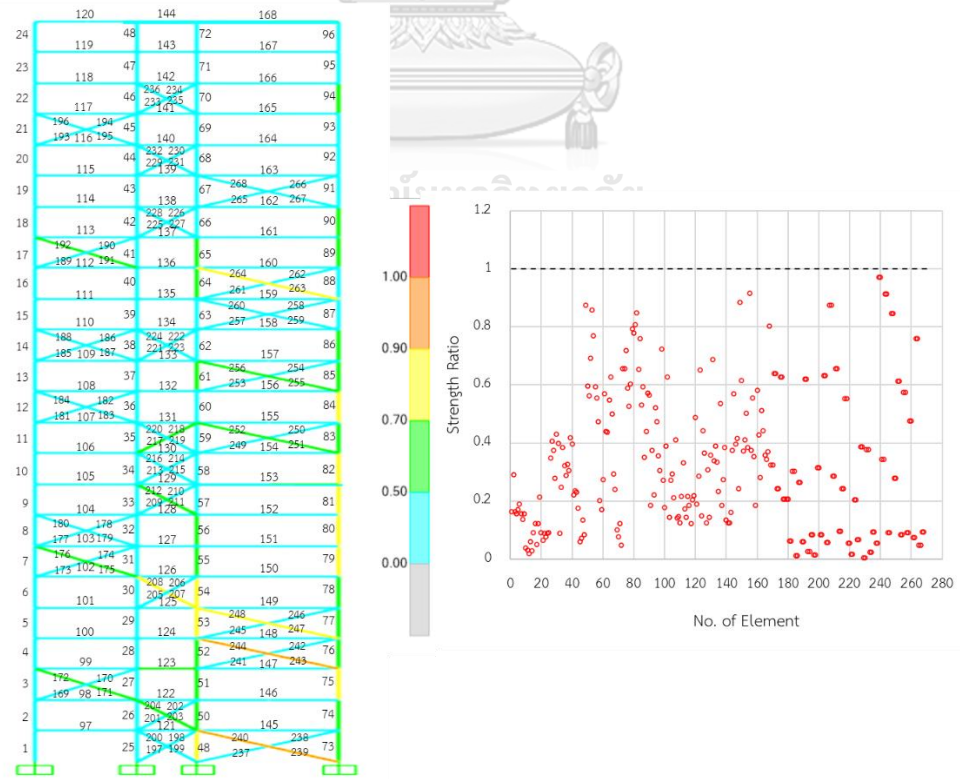


Figure 5.19 Element strength ratio for three-bays, twenty-four-stories frame (No.2)

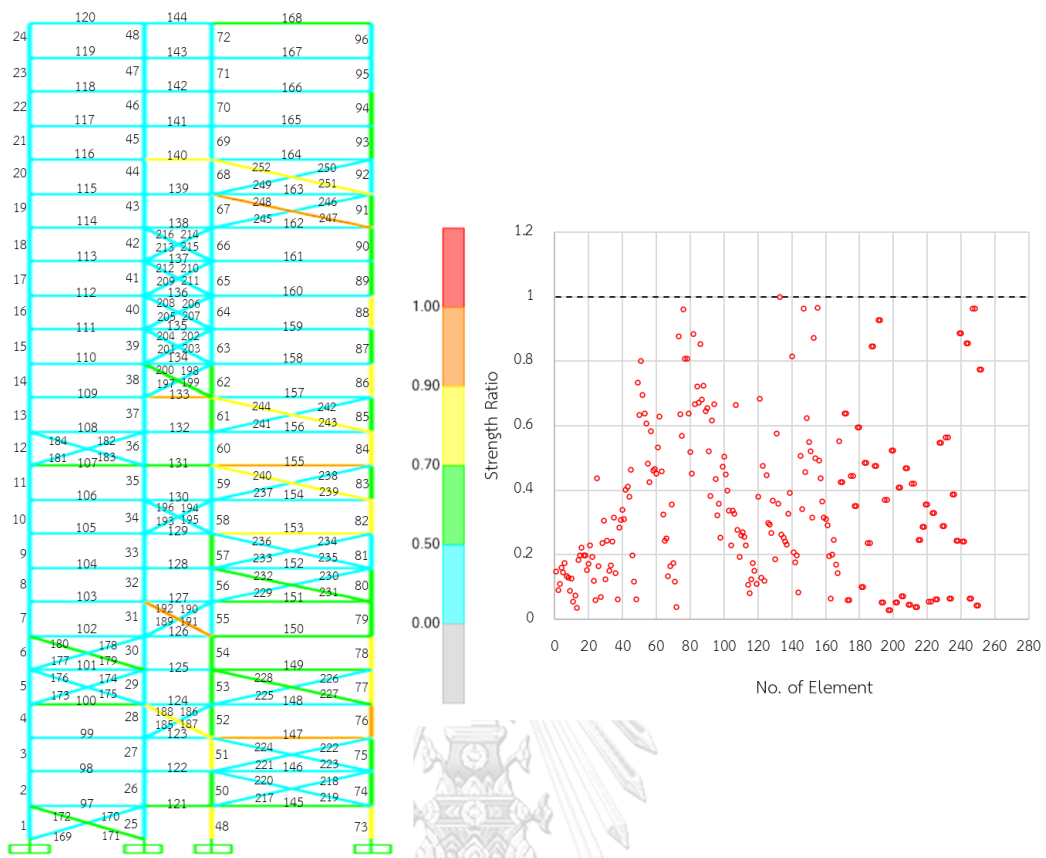


Figure 5.20 Element strength ratio for three-bays, twenty-four-stories frame (No.3)

Unbrace frame considers drift for all stories. BPSO is compared with HS, TLBO and SBO. BPSO gets almost the worst weight, which is 205,056. The weight is greater than TLBO and SBO and less than HS. It should be noted that TLBO has not any information of runtimes. The maximum strength ratio is 0.9221, which happened in the right end column of the 13th story. The maximum drift ratio is 0.9999, which happened in the 4th story. The minimum weight of the brace frame using the original grouping (Frame No.2) is 132,972 lb. This weight is lower than the unbraced frame with the same grouping, 35.15%. The maximum strength ratio is 0.9722, which happened the right bracing of 1st story. The maximum drift ratio is 0.9999, which happened in the 23rd story. For the braced frame with finer grouping (Frame No.3), the minimum weight is 138,050 lb greater than the braced frame's minimum weight with the original grouping of 3.82%. The maximum strength ratio is 0.9999, which happened in the middle beam of story 13th. The maximum drift ratio is 0.9999, which happened in 21rd story.

CHAPTER 6

CONCLUSION AND FUTURE WORK

6.1 Conclusion

This research applies BPSO to solve steel structural weight optimization problems. The research studies on varying inertia weight of BPSO in value and pattern to find the best inertia weight improving the algorithm performance. The samples of study include constant inertia weight 0.9, 0.92, 0.94, 0.96, 0.98, 1.00 and 1.02 and linear decreasing inertia weight from 0.9 to 0.4. The samples experiment on six benchmark mathematic optimization functions. The best inertia weight from the sample is applied in the algorithm for the structural weight optimizations. There are two types of structures studied under drift and strength constrained function by AISC, unbraced structure and braced structure. From the experiment, the result can be concluded as follows:

- 1) The best inertia weight among the sample is constant inertia weight 0.98. The inertia weight is the best in both accuracy and precision term. So, this value is applied in the BPSO algorithm to optimize the structural optimization problem.
- 2) The first structure is a two-bay, three-stories structure. The result from the BPSO algorithm is compared to GA, ACO, and SBO algorithms. All practical algorithms can reach the optimal value. But BPSO is the best one with full percentage success and using the shortest iteration for getting minimum value.

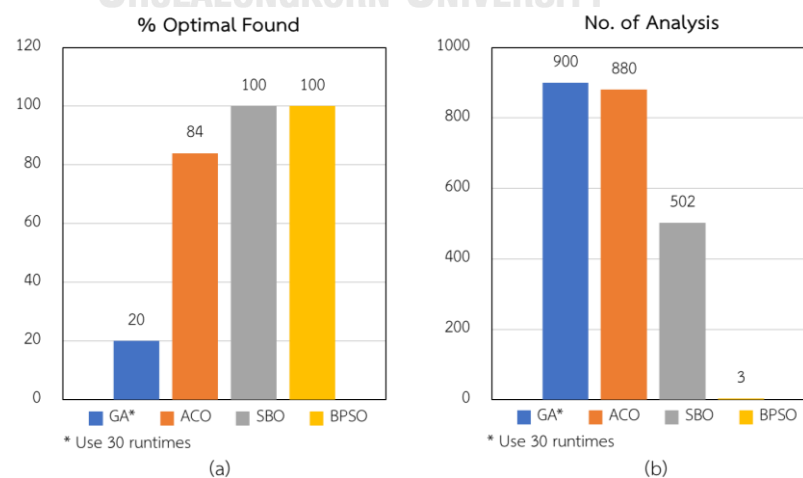


Figure 6.1 Two-bay, three-stories frame (a) % optimal found from total runtimes (b) No. of analysis getting minimum weight

3) The second structure of testing is a one-bay, ten-stories structure. Two unbraced frames can reach the lowest weight comparing with other algorithms. The algorithms have the highest standard deviation but the fastest convergence. The braced frame with initial grouping can get a lower weight than unbrace frame with the same grouping. The structure weight is decreased when classifying braced frame with finer grouping.

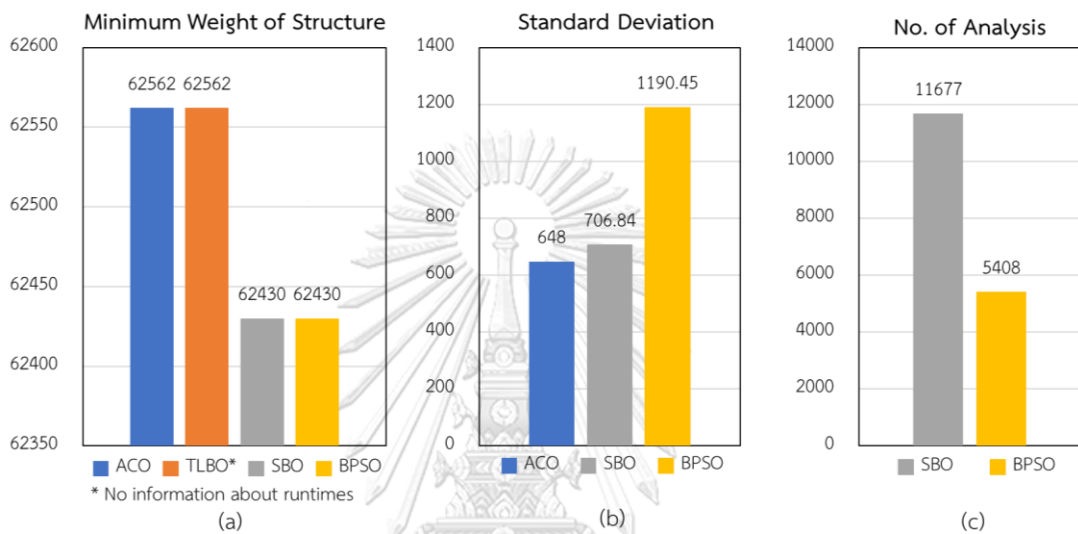


Figure 6.2 Unbraced one-bay, three-stories frame considering drift at roof (a) minimum weight (b) standard deviation of weight for total runtimes (c) No. of analysis getting minimum weight

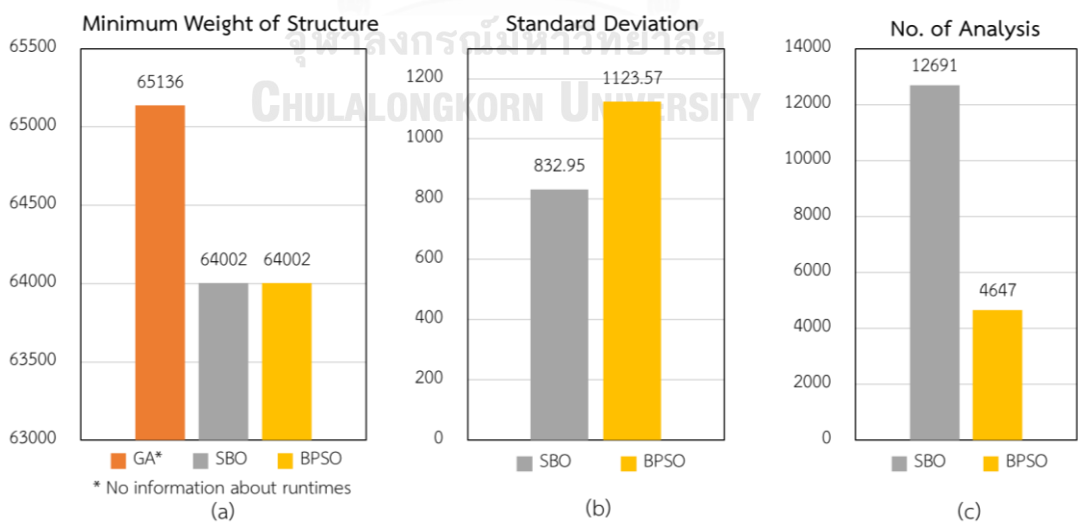


Figure 6.3 Unbraced one-bay, three-stories frame considering drift for all stories (a) minimum weight (b) standard deviation of weight for total runtimes (c) No. of analysis getting minimum weight

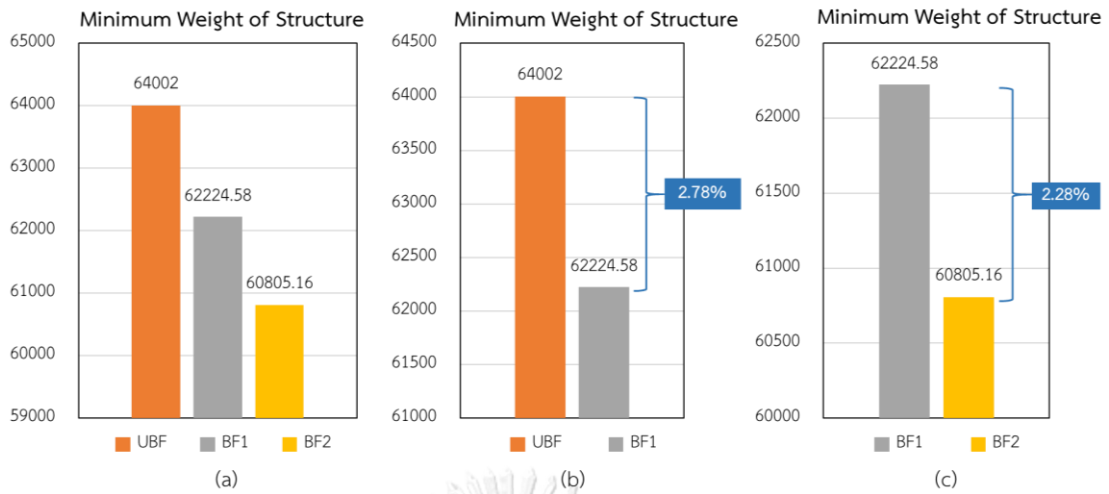


Figure 6.4 minimum weight for all types of one-bay, twenty-four-stories frame

4) The second structure of testing is a three-bay, twenty-four-stories structure. Unbraced frame gets the second heavier weight comparing with the other three algorithms. The braced frame with initial grouping can get a lower weight than unbrace frame with the same grouping. The structure weight is increased when classifying braced frame with finer grouping.

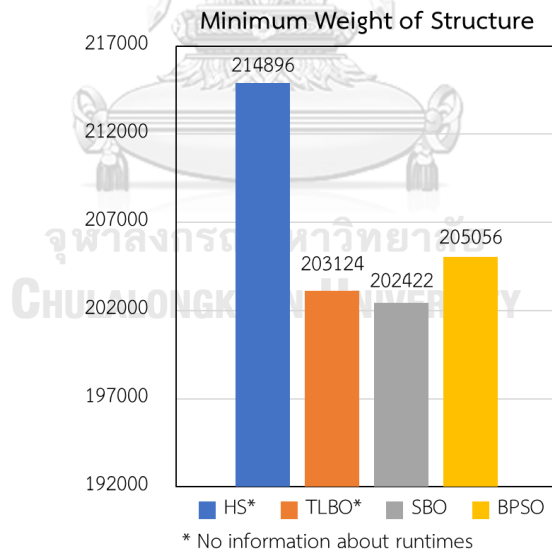


Figure 6.5 Minimum weight of unbraced frame of three-bay, twenty-four-stories frame

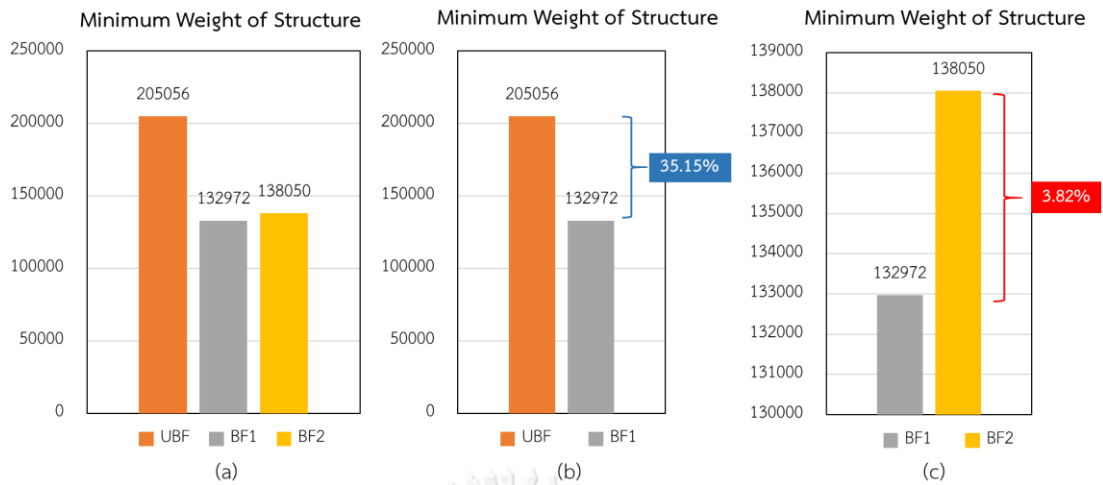


Figure 6.6 Minimum weight for all types of each three-bay, twenty-four-stories frame

5) For comparison three bay, twenty-four stories unbraced frame using BPSO and other algorithms, BPSO get bad result. When we consider the convergence curve, BPSO converges so fast with only 6,890 No. of analysis. It can conclude that BPSO may be stuck in a local optimum. The study of structure types for one-bay with ten-stories frame and three-bays, twenty-four-stories frames shows the contradictory result. From example two, BPSO can be found the lower weight when the elements have more grouping. This is reasonable that when the grouping is finer divided, the optimization can get the lower weight due to the independence of element selection. However, the third example cannot reach this way. When dividing to finer grouping, the weight we got is higher. When we consider the number of analyses, it is found that the number of analyses is so close to the maximum iteration. It is possible that BPSO is still not converted and reaches the optimal value it can find. Another guess is that BPSO stuck with the local optimum due to seeing the unbraced frame compared to other algorithms. BPSO almost had the worst result.

6.2 Future Work

From the conclusion part, it is still bad result and contradictory in BPSO study. To find the cause of problem, it is necessary to test more about the influence of parameters as following:

1. BPSO algorithm may be stuck in local optimum in some examples. So, a constant inertia weight of 0.98 cannot find an optimal solution. We suggest

future work studying the inertia weight with different values and patterns such as linear increasing inertia weight to find the better inertia weight

2. Other BPSO parameters such as the number of populations, initial parameters, maximum velocity, and acceleration coefficient may significantly influence BPSO performance. Future work may study on varying these parameters.
3. From considering three bay, twenty-four stories braced frame, No. of analysis to get minimum weight is so close to maximum iteration. Future work may study these frames with larger maximum iteration to see their truly minimum weight.
4. According to using a binary system in BPSO, the search space in BPSO is larger than other algorithms due to fake available solutions for fulfilling available solutions of the binary system. These fake available solutions may affect the nonlinearity of function that makes BPSO stuck in a local optimum. Future work may study on setting the value of fake available solutions.
5. This research design structure bases on the effect of the second-order effect. However, AISC specification has other requirements to design for the stability of structure. The future study may focus on structural optimization problems, including the design for stability requirement by AISC using BPSO compare with other algorithms such as ESO (Chaiwongnoi et al., 2020).

REFERENCES

- AISC. (2011). *Steel Construction Manual*: American Institute of Steel Construction, Chicago, IL.
- AISC. (2016). *Specification for Structural Steel Buildings (ANSI/AISC 360-16)*: American Institute of Steel Construction, Chicago, IL.
- Camp, C., Bichon, B., & Stovall, S. (2005). Design of Steel Frames Using Ant Colony Optimization. *Journal of Structural Engineering*, 131. doi:10.1061/(ASCE)0733-9445(2005)131:3(369)
- Chaiwongnoi, A., Van Thu, H., Tangaramvong, S., & Van, C. N. (2020). *An ESO Approach for Optimal Steel Structure Design Complying with AISC 2010 Specification*. Paper presented at the International Conference on Green Technology and Sustainable Development.
- Davison, J. H., & Adams, P. F. (1974). Stability of Braced and Unbraced Frames. *Journal of the Structural Division*, 100(2), 319-334.
- Degertekin, S. O. (2008). Optimum Design of Steel Frames using Harmony Search Algorithm. *Structural and Multidisciplinary Optimization*, 36(4), 393-401.
- Eberhart, R., & Kennedy, J. (1995, 4-6 Oct. 1995). *A New Optimizer Using Particle Swarm Theory*. Paper presented at the MHS'95. Proceedings of the Sixth International Symposium on Micro Machine and Human Science.
- Farshchin, M., Maniat, M., Camp, C. V., & Pezeshk, S. (2018). School Based Optimization Algorithm For Design of Steel Frames. *Engineering Structures*, 171, 326-335.
- Feiring, B. R., Phillips, D. T., & Hogg, G. L. (1985). Penalty Function Techniques: A Tutorial. *Computers & Industrial Engineering*, 9(4), 307-326. doi:10.1016/0360-8352(85)90019-1
- Guo, S.-s., Wang, J.-s., & Guo, M.-w. (2020). Z-Shaped Transfer Functions for Binary Particle Swarm Optimization Algorithm. *Computational Intelligence and Neuroscience*, 1-21. doi:10.1155/2020/6502807
- Haque, A. U., Atik, M., Muhtadi, R., & Zasiah, T. (2018). *Effect of Different Bracing Systems on The Structural Performance of Steel Building*. Paper presented at

- the 4th International Conference on Civil Engineering for Sustainable Development, Khulna, Bangladesh.
- Jagdish, J., & Doshi, T. D. (2013). A Study on Bracing Systems on High Rise Steel Structures. *International Journal of Engineering Research and Technology*, 2, 1672-1676.
- Kennedy, J., & Eberhart, R. C. (1997, 12-15 Oct. 1997). *A Discrete Binary Version of The Particle Swarm Algorithm*. Paper presented at the 1997 IEEE International Conference on Systems, Man, and Cybernetics. Computational Cybernetics and Simulation.
- McGuire, W., Gallagher, R. H., & Saunders, H. (1982). *Matrix Structural Analysis*.
- Mirjalili, S., & Lewis, A. (2013). S-shaped versus V-shaped Transfer Functions for Binary Particle Swarm Optimization. *Swarm and Evolutionary Computation*, 9, 1-14. doi:10.1016/j.swevo.2012.09.002
- Mirjalili, S., Wang, G.-G., & Coelho, L. d. S. (2014). Binary Optimization Using Hybrid Particle Swarm Optimization and Gravitational Search Algorithm. *Neural Computing and Applications*, 25(6), 1423-1435. doi:10.1007/s00521-014-1629-6
- Pezeshk, S., Camp, C., & Chen, D. (2000). Design of Nonlinear Framed Structures Using Genetic Optimization. *Journal of Structural Engineering*, 126. doi:10.1061/(ASCE)0733-9445(2000)126:3(382)
- Poli, R., Kennedy, J., & Blackwell, T. (2007). Particle Swarm Optimization. *Swarm Intelligence*, 1(1), 33-57. doi:10.1007/s11721-007-0002-0
- Shi, Y., & Eberhart, R. (1998). *A Modified Particle Swarm Optimizer*. Paper presented at the 1998 IEEE International Conference on Evolutionary Computation Proceedings. IEEE World Congress on Computational Intelligence (Cat. No.98TH8360).
- Tang, K., Li, X., Suganthan, P., Yang, Z., & Weise, T. (2009). *Benchmark Functions for The CEC'2008 Special Session and Competition on Large Scale Global Optimization* (Vol. 1).
- Toğan, V. (2012). Design of Planar Steel Frames Using Teaching–Learning Based Optimization. *Engineering Structures*, 34, 225–232. doi:10.1016/j.engstruct.2011.08.035

Wood, B. R., Beaulieu, D., & Adams, P. F. (1976). Column Design by P Delta Method.
Journal of the Structural Division, 102(2), 411-427.





จุฬาลงกรณ์มหาวิทยาลัย
CHULALONGKORN UNIVERSITY

VITA

NAME Atitaya Chaiwongnoi

DATE OF BIRTH 12 July 1996



จุฬาลงกรณ์มหาวิทยาลัย
CHULALONGKORN UNIVERSITY